

BIOPROCESS DEVELOPMENT FOR RECOMBINANT THERAPEUTIC PROTEIN  
OSTEOPONTIN FROM ESCHERICHIA COLI

A Thesis

by

SHENGCHUN GUO

Submitted to the Office of Graduate and Professional Studies of  
Texas A&M University  
in partial fulfillment of the requirements for the degree of

MASTER OF SCIENCE

Chair of Committee,	Zivko Nikolov
Committee Members,	Arul Jayaraman
	Carmen Gomes
Head of Department,	Stephen Searcy

May 2018

Major Subject: Biological and Agricultural Engineering

Copyright 2018 Shengchun Guo

## ABSTRACT

Osteopontin (OPN) is a multifunctional protein presented in various organs and body fluids in human body. OPN serves important roles in bone remodeling, wound healing, and other biomineralization related physiological activities, which gives it great potential health benefits. Clinical statistics and laboratory researches also indicate that OPN can be a suitable diagnostic and prognostic marker for cancer progression. Its role in cell signaling remains one of the hot topics in biomedicine research. However, there was no efficient and scalable process for OPN purification from recombinant sources reported, which prevents OPN unleashing its full potential in health industry. Low expression level, acidic isoelectric point, and the lack of well-defined secondary and tertiary structure are some of the challenges that faced purification development of OPN from *Escherichia coli* (*E. coli*) lysates. Finding an adequate capture step with sufficient specificity and binding capacity that could be paired with an orthogonal purification step was a vitally important objective for this project.

In recent years, mixed-modal chromatography (MMC) resins have opened up new possibilities for protein purification. The combination of high-throughput screening (HTS) platforms and design of experiment (DOE) principles could accelerate process development exponentially.

In this research, seven chromatography resins including traditional ion exchange resin, hydrophobic interaction resin and 5 mixed-modal resins were screened for OPN purification. Plate based HTS was applied and quickly revealed comprehensive information about the affinity between the ligands and the target protein, specificity of

the adsorption, and the binding capacity of the resins. Based on HTS results, the bind/elute processes for all candidate resins were designed, tested and optimized with small scale batch adsorption experiments. The purification factors and OPN recoveries achieved by batch adsorption experiments were verified on packed-bed columns operated by ÄKTA system and analyzed statistically. In terms of purification factor and yield, HEA HyperCel and Capto Q performed significantly better than the rest of the candidate resins. Two 2-step purification processes assembled with these two resins elevated OPN purity from 2% from the lysate to over 95% purity with greater than 40% yield.

## ACKNOWLEDGEMENTS

I would like to thank my committee chair, Dr. Zivko L. Nikolov, for his inspiration, support, supervision, and encouragement. I would extend my thanks to my committee members, Dr. Arul Jayaraman and Dr. Carmen Gomes, for their guidance and support throughout the course of this research.

I would like to acknowledge the funding of this work by the National Science Foundation (Chemical, Bioengineering, Environmental, and Transport Systems Grant #1160117). A thank you to Dr. Stephen Mayfield and his group, at the University of California San Diego, for providing transgenic strains of *E. coli*.

I would thank my colleagues from the Bioseparations lab for keeping a lively environment to work and making my research such an enjoyable adventure. Thanks also go to my friends and the department faculty and staff for making my time at Texas A&M University a great experience.

Finally, thanks to my mother and father for their encouragement, patience and unconditional love.

## CONTRIBUTORS AND FUNDING SOURCES

### **Contributors**

This work was supported by a thesis committee consisting of Professor Zivko L. Nikolov [advisor] and Professor Carmen Gomes of the Department of Biological and Agricultural Engineering and Professor Arul Jayaraman from the Department of Chemical Engineering.

The starting material for this work specified in section 2.1 was provided by Dr. Stephen Mayfield and his group from the University of California San Diego.

All other work conducted for the thesis was completed by the student independently.

### **Funding Sources**

This work was funded by the National Science Foundation (Chemical, Bioengineering, Environmental, and Transport Systems Grant #1160117).

## NOMENCLATURE

AS	Ammonia Sulfate
BSA	Bovine serum albumin
CV	Column volume
DBC	Dynamic binding capacity
<i>E. coli</i>	<i>Escherichia coli</i>
ELISA	Enzyme-linked immunosorbent assay
FPLC	Fast protein liquid chromatography
HCP	Host cell protein
HIC	Hydrophobic interaction chromatography
HRP	Horseradish peroxidase enzyme
HTS	High-throughput screening
IEX	Ion exchange chromatography
MMC	Mixed-modal chromatography
MWCO	Molecular weight cut-off
NaCl	Sodium Chloride
NaP	Sodium phosphate
OPN	Osteopontin
PBS	Phosphate-buffered saline
PES	Polyethersulfone
pI	Isoelectric point
PMSF	Phenylmethane sulfonyl fluoride

PTM	Post-translational modification
REML	Residual maximum likelihood
RO	Reverse osmosis
SDS-PAGE	sodium dodecyl sulfate polyacrylamide gel electrophoresis
TMB	3,3',5,5'-Tetramethylbenzidine
TP	Total protein
Tris	Tris (hydroxymethyl) aminomethane

## TABLE OF CONTENTS

	Page
ABSTRACT .....	ii
ACKNOWLEDGEMENTS .....	iv
CONTRIBUTORS AND FUNDING SOURCES.....	v
NOMENCLATURE.....	vi
TABLE OF CONTENTS .....	viii
LIST OF FIGURES.....	x
LIST OF TABLES .....	xiii
1 INTRODUCTION AND LITERATURE REVIEW .....	1
1.1 Introduction.....	1
1.2 Literature review .....	2
1.2.1 Osteopontin(OPN) properties and roles in body fluids.....	2
1.2.2 <i>Escherichia coli</i> ( <i>E. coli</i> ) expression system and recombinant OPN.....	5
1.2.3 Protein purification by chromatography .....	8
1.2.4 OPN purification methods.....	16
2 MATERIALS AND METHODS.....	20
2.1 <i>E. coli</i> cell cultivation and harvest.....	20
2.2 Cell lysis and protein extraction .....	20
2.3 High-throughput screening (HTS) of mixed-modal sorbents .....	21
2.4 Batch adsorption and elution of OPN .....	22
2.5 Packed-bed purification of OPN.....	27
2.6 Analytical methods .....	29
2.6.1 Bradford assay for total protein (TP) determination .....	29
2.6.2 ELISA (enzyme-linked immunosorbent assay) for OPN quantification .....	30
2.6.3 SDS- PAGE and Western- blot for product quality measurement.....	30
2.7 Resin performance evaluation .....	31
2.8 Statistical analysis.....	32
2.8.1 Response surface analysis for HTS results .....	32
2.8.2 Least square fitting for resin comparison .....	32



3	RESULTS AND DISCUSSION .....	34
3.1	Resin adsorption and elution studies .....	34
3.1.1	OPN adsorption and elution studies with anion exchange resin (Capto Q) ...	34
3.1.2	OPN adsorption and elution studies with a hydrophobic interaction resin (Phenyl Sepharose).....	36
3.1.3	OPN adsorption and elution studies with ceramic hydroxyapatite (CHT).....	38
3.1.4	OPN adsorption and elution studies with mixed-modal resins .....	40
3.1.5	Resin performance evaluation and comparison .....	52
3.1.6	Resin performance verification and optimization on packed-bed columns ...	56
3.2	Two-step OPN purification process design .....	60
3.2.1	OPN purification by HEA-Q process .....	60
3.2.2	OPN purification by Q-HEA process .....	65
4	CONCLUSION AND RECOMMENDATIONS .....	67
4.1	Conclusion .....	67
4.2	Recommendation .....	69
	REFERENCES .....	70
	APPENDIX .....	78

## LIST OF FIGURES

	Page
Figure 1 Model of human OPN (Reprint from Kazanecki et al. 2007 <sup>9</sup> ) .....	3
Figure 2 Surface charge prediction of OPN, plotted from prediction generated by ProtCalculator v3.4 (ProtCalc.net) .....	11
Figure 3 Hydrophobicity of HIC resins (Reprint from GE Healthcare Lifesciences <sup>34</sup> )..	12
Figure 4 Batch adsorption and elution of OPN and total protein (TP) on anion exchange resin (Capto Q). Adsorption condition was 50 mM Tris buffer at pH 7. Elution steps were conducted with 50 mM Tris, pH 7 containing 0.2 M, 0.5 M, and 1 M NaCl, respectively. The data reported were percentage normalized against the amount in the feed. The adsorption experiments were performed in triplicate and bars represent the standard deviation. ....	36
Figure 5 Batch adsorption and elution of OPN and <i>E. coli</i> total proteins by HIC (Phenyl Sepharose). Adsorption was done from conditioned <i>E. coli</i> lysate which contained 1.0 M ammonium sulfate at pH 7. Elution steps were 0.5 M ammonium sulfate and 0 M ammonium sulfate. All solutions in this experiment were buffered by 50 mM Tris at pH 7. The data reported were percentage normalized against the amount in the feed. The adsorption experiments were performed in triplicate. Bars represent the standard deviation. ....	38
Figure 6 Batch adsorption and elution of OPN and total proteins (TP) using ceramic hydroxyapatite. Adsorption was performed from <i>E. coli</i> clarified lysate dialyzed against 5 mM sodium phosphate buffer at pH 6.8. Elution 1: 0.1 M sodium phosphate buffer pH 6.8; Elution 2: 0.2 M sodium phosphate buffer pH 6.8. ....	39
Figure 7 Contour profile of OPN (A) and total protein (B) bound to HEA HyperCel. Numbers on the contour grids represent the fraction of protein in the lysate that was adsorbed to HEA Hypercel.....	41
Figure 8 Low-salt batch adsorption and elution of OPN and <i>E. coli</i> total proteins using HEA HyperCel: Adsorption was performed from pH 7 <i>E. coli</i> clarified lysate containing 150 mM. Elution steps are pH 7 with 1 M NaCl, pH 5 with 1 M NaCl, and pH 3 with no NaCl addition. ....	43
Figure 9 High-salt batch adsorption and elution of OPN and <i>E. coli</i> total soluble protein using HEA HyperCel: Adsorption was performed from conditioned	

	<i>E. coli</i> clarified lysate with 3 M NaCl pH7. Elution steps were pH 7 with 1 M NaCl, pH 5 with 1 M NaCl, and pH 3 with no NaCl addition. ....	44
Figure 10	Contour profile of the proportion of OPN (A) and total protein (B) bound to PPA HyperCel. Numbers on the contour grids represent the fraction of protein in the lysate that was adsorbed to PPA HyperCel. ....	45
Figure 11	Low-salt batch adsorption and elution of OPN and <i>E. coli</i> total soluble protein using PPA HyperCel: Adsorption was performed from <i>E. coli</i> clarified lysate containing 150 mM NaCl pH 7. Elution steps were pH 7 with 1 M NaCl, pH 5 with 1 M NaCl, and pH 3 with no NaCl addition. ....	46
Figure 12	High-salt batch adsorption and elution of OPN and <i>E. coli</i> total protein using PPA HyperCel: Adsorption was performed from conditioned <i>E. coli</i> clarified lysate containing 3 M NaCl at pH 7. Elution steps are pH 7 with 1 M NaCl, pH 5 with 1 M NaCl, and pH 3 with no NaCl addition. ....	47
Figure 13	Contour profile of the proportion of OPN (A) and total protein (B) bound to Capto adhere. Numbers on the contour grids represent the fraction of protein in the lysate bound to the Capto adhere. ....	48
Figure 14	Batch adsorption and elution of OPN and <i>E. coli</i> total soluble protein by Capto adhere, <i>E. coli</i> clarified lysate was dialyzed to remove salt before adsorption. Binding condition: pH 7 50 mM Tris Buffer. Elution 1 - 3: Citrate-phosphate buffer pH 5, pH 4, pH 3. ....	49
Figure 15	Batch adsorption and elution of OPN and <i>E. coli</i> total protein using MEP HyperCel: Adsorption was performed from pH 7 <i>E. coli</i> clarified lysate containing 3 M NaCl. Elution steps are pH 7 with 1 M NaCl, pH 5 with 1 M NaCl, and pH 3 without NaCl addition. ....	51
Figure 16	Chromatogram of HEA HyperCel low salt bind/elute operated by ÄKTA system. OPN eluted in the peak around 1 M NaCl illustrated between the red-dotted lines. ....	57
Figure 17	Chromatogram of anion exchange chromatography. Dialyzed <i>E. coli</i> lysate loaded on HiScreen Capto Q column. Elution by ascending NaCl concentration linear gradient. OPN eluted between 0.26 M and 0.45 M NaCl illustrated between the red-dotted lines. ....	58
Figure 18	Chromatogram of HEA HyperCel low-salt binding and step elution. The elution peak was collected for Capto Q purification (23-31 ml). ....	61
Figure 19	Chromatogram of OPN purification on Capto Q following HEA HyperCel capture. ....	63

Figure 20 Purification of OPN by HEA and Capto Q two-step process. A: SDS-PAGE with Coomassie stain (SimpleBlue™ SafeStain); B: Western-blot image. Both images are from the identical gel with the same sample loading in each lane. Lane 1: molecular weight markers; lane 2: *E. coli* clarified lysate; lane 3: Partially purified OPN fraction from HEA HyperCel elute; lane 4: Dialyzed HEA purified fraction as the feed for Capto Q chromatography; lane 5: Capto Q elute pool. For lane 2-5, total protein loading was kept constant at 5 µg/lane. ....64

Figure 21 Purification of OPN by Q-HEA process SDS-PAGE (A) with Coomassie stain (SimpleBlue™ SafeStain) and Western-blot ((B) images. Lane 1: molecular weight marker; lane 2: *E. coli* clarified lysate; lane 3: Partially purified OPN fraction from Capto Q elute; lane 4-6: OPN elute fractions from HEA HyperCel. ....66

## LIST OF TABLES

	Page
Table 1 List of biopharmaceuticals produced in <i>E. coli</i> (Reprint from Beashen et al. 2015 <sup>29</sup> ) .....	6
Table 2 List of commonly used ion exchangers for protein purification .....	10
Table 3 List of mixed-modal resins (Reprint from Zhao et al. 2009 <sup>47</sup> ) .....	15
Table 4 List of candidate chromatography sorbents for OPN purification. ....	23
Table 5 Effect of ammonium sulfate addition to <i>E. coli</i> lysate on OPN and TP loss due to precipitation. The pellets formed by ammonium sulfate precipitation were removed by centrifugation. OPN and TP recovery in the supernatant and enrichment factors of ammonium sulfate were listed. (The experiments were done in triplicates; data shown with the standard deviation) .....	37
Table 6 Comparison of resins by batch purification experiments, their respective purification factors and recoveries. Recovery and purification factors are expressed as mean $\pm$ standard deviation. Values having the same letters are not significantly different. ....	55
Table 7 Purification of OPN from <i>E. coli</i> lysate by HEA-Q 2-step process .....	64
Table 8 Purification of OPN from <i>E. coli</i> lysate by Q-HEA 2-step process .....	66

# 1 INTRODUCTION AND LITERATURE REVIEW

## 1.1 Introduction

Osteopontin (OPN) is a protein essential for bone remodeling, wound healing, and inhibition of kidney stone formation. It also plays important roles in cell signaling pathways and cell migration activities in regular conditions and stress responses, which makes OPN a suitable molecular marker for cancer cell types and cancer progression. The potential health benefits as well as potential diagnostic and prognostic value of OPN have invigorated the search for an efficient and scalable purification process. Although OPN was identified and isolated in the 1980s<sup>1-3</sup>, there has not been a feasible process reported for large scale OPN production. Ion exchange and hydrophobic interaction chromatography methods have been used for OPN purification from native and recombinant sources, however, most of the reported purification processes suffered from low yield and poor scale-up capabilities<sup>4-5</sup>. The lack of efficient OPN purification strategies for large scale production hindered OPN from unleashing its full potential in the health industry.

As new technologies for downstream processing are being developed, it is time to revisit the challenge of OPN purification. Recently, mixed-modal chromatography (MMC) resins have caught attention for their wide range of adsorption chemistries and unique features compared to traditional single mode resins. And 96-well plate based high-throughput screening technologies (HTS) combining with statistics can exponentially accelerate resin-protein interaction studies, resin screening and process optimization.

In this project, high-throughput process development strategy was implemented to the design of a robust, efficient, and scalable OPN purification process.

## **1.2 Literature review**

### *1.2.1 Osteopontin(OPN) properties and roles in body fluids*

OPN is a multifunctional protein present in a wide variety of mammalian organs and tissues. Studies on its physical and chemical properties and functions in various biochemistry processes are being reported on a regular basis.

OPN is single polypeptide composed of about 300 amino acids. The backbone molecular weight is 33 kDa. However the apparent molecular weight can range from 45 kDa to 75 kDa when analyzed by SDS-PAGE due to the posttranslational modification and its high negative charge<sup>6</sup>. OPN is highly acidic with an isoelectric point at about 4.3<sup>1</sup>. OPN is often categorized as a Intrinsically Disordered Protein (IDP) which is biologically active in an flexible form lacking a well-defined secondary and tertiary structure<sup>7-8</sup>. As shown in Figure 1, OPN has a polyaspartic acids motif which serves as calcium binding sites and an arginine-glycine-aspartic acid (RGD) domain that binds to integrins and promotes cell migration and adhesion activities.

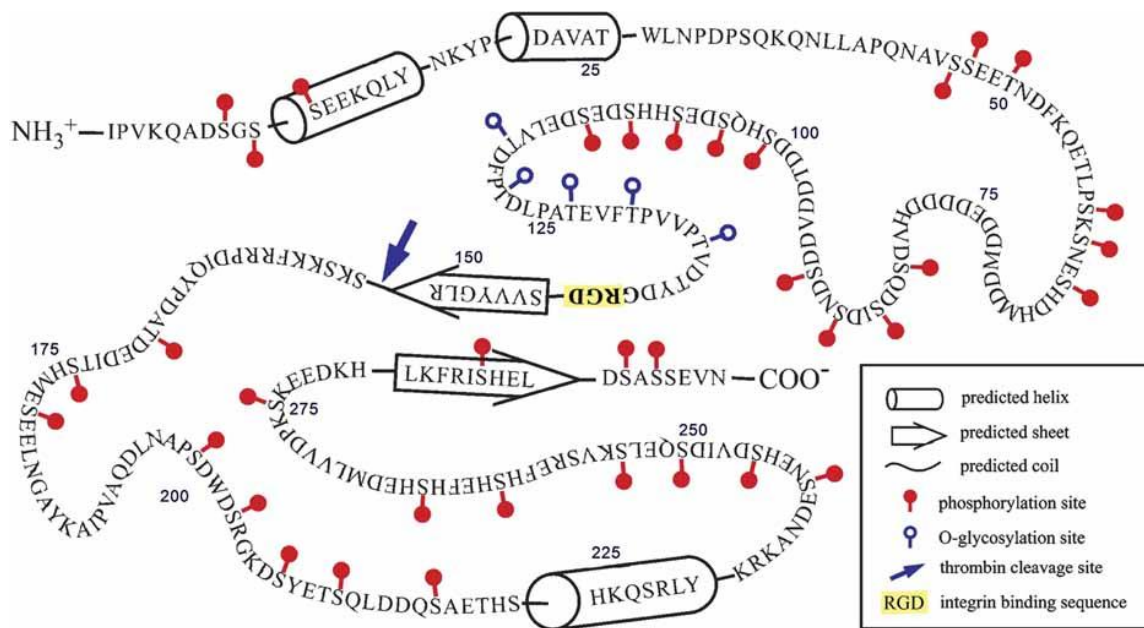


**Figure 1** Model of human OPN (Reprint from Kazanecki et al. 2007<sup>9</sup>)

OPN undergoes extensive posttranslational modification (PTM) events in the bone and other tissues. Bovine mammary gland OPN has 3 *O*-glycosylation and 28 phosphorylation sites<sup>10</sup>. Human milk OPN has 5 *O*-glycosylation and 29 phosphorylation sites<sup>11</sup>. Phosphorylations on OPN often appear in clusters and the extent of phosphorylation varies with the issue OPN was expressed in. OPN serves various functions which will be discussed in the following sections.

OPN is highly expressed in the bone. Its function in bone formation and calcification was first discovered in 1989<sup>12</sup>. OPN is highly enriched in the mineralization front anchoring Osteoclasts to the mineral matrix of bones<sup>13</sup>. Later research revealed that OPN acts as a mediator of cell-matrix and matrix-matrix adhesion in the formation and repair process of regular or pathological mineralized tissues<sup>14</sup>. The calcium binding sites allows OPN tightly binds to hydroxyapatite—the major inorganic component of bone



matrix. The RGD domain in the middle of OPN sequence provides an integrin binding site which living cells attach to and facilitate their mobility<sup>15</sup>. OPN knock-out mice model helped researchers uncovered the importance of OPN in bone development as OPN knock-out mice developed hyper-mineralized bones and suffer from high fragility and deficiency of stress-induced bone remodeling<sup>16</sup>.

The biomineralization function of OPN does not stop within the bone. OPN plays an important role in the inhibition of renal stones which are mostly composed of calcium salts. Urine is often supersaturated with respect to calcium oxalate but most people do not form stones. OPN is one of the many biological macromolecules that prohibit the aggregation of calcium oxalate thus preventing the nucleation and growth of renal stones. OPN is synthesized and secreted in the kidney by epithelial cells<sup>17-18</sup>.

Experiments both *in vitro* and *in vivo* show direct evidence that OPN inhibit calcium crystal formation<sup>19-20</sup>. OPN can be found in urine with concentration ranging from 1.9 to 4.3  $\mu\text{g/ml}$ . The lower limit of OPN sufficient for the inhibition of calcium oxalate aggregation is reported to be 1.9  $\mu\text{g/ml}$ <sup>19</sup>. One study reported that single base mutation in OPN gene was identified from patients with recurrent stone formation or familial urolithiasis<sup>21</sup>.

Besides its functions in biomineralization and related health benefits, OPN is also involved in cell signaling and cancer progression. OPN expression is significantly up-regulated in cancer cells compared with normal tissue cells in at least 30% of cancer patients<sup>22</sup>. L. Shevde<sup>23</sup> did a good job reviewing the roles OPN plays in cancer progression. OPN expression level and its post-translational modification are highly

correlated with cancer cell types and tumor stages, so it could serve as a valuable marker for cancer prognosis and diagnosis<sup>24-25</sup>.

Moreover, studies about the functionality of OPN in cell signaling and cancer progression are being reported on a regular basis, which makes it vitally important to have a robust way to produce full-length OPN free from variation introduced by post-translational modification for related research purposes and anti-body development.

### 1.2.2 *Escherichia coli* (*E. coli*) expression system and recombinant OPN

*E. coli* is one of the most widely applied and well-studied expression systems for recombinant protein production. The first recombinant DNA was transferred to *E. coli* cells in 1973<sup>26</sup> and the FDA approved *E. coli* recombinant human insulin for the diabetes treatment which is the first recombinant pharmaceutical entering the market<sup>27-28</sup>. Since then, *E. coli* produced pharmaceuticals took off in the market and remains the major work horse in the biopharmaceutical industry producing 30% of approved therapeutic proteins in the market<sup>29</sup>. Although increasing numbers of biopharmaceuticals from mammalian cell lines have been approved, quantitatively speaking, microbial systems continues to dominate the market as 17.9 metric tons of active biopharmaceutical ingredient (68%) being derived from microbial systems<sup>30</sup> with *E. coli* expressed protein products being the major contributor. Human insulin alone contributed more than 6 metric tons of production annually. And recombinant insulin from Ely Lilly alone generated revenue of \$1.366 billion for the company in 2016 according to its annual financial report. Table 1 is a list of biopharmaceuticals from *E. coli* approved to enter the market.

**Table 1** List of biopharmaceuticals produced in *E. coli* (Reprint from Beashen et al. 2015<sup>29</sup>)

<b>Biologic</b>	<b>Therapeutic Indication</b>	<b>Year of Approval</b>	<b>Company</b>
<b>Humulin (rh insulin)</b>	Diabetes	1982 US	Eli Lilly
<b>IntronA (interferon <math>\alpha</math>2b)</b>	Cancer, hepatitis, genital warts	1986 US	Schering-Plough
<b>Roferon (interferon <math>\alpha</math>2a)</b>	Leukemia	1986 US	Hoffmann-La-Roche
<b>Humatrope (somatropin rh growth hormone)</b>	hGH deficiency in children	1987 US	Eli Lilly
<b>Neupogen (filgrastim)</b>	Neutropenia	1991 US	Amgen Inc.
<b>Betaferon (interferon <math>\beta</math>-1b)</b>	Multiple sclerosis	1993 US	Schering Ag
<b>Lispr (fast-acting insulin)</b>	Diabetes	1996 US	Eli Lilly
<b>Rapilysin (reteplase)</b>	Acute myocardial infarction	1996 US	Roche
<b>Infergen (interferon alfacon-1)</b>	Chronic hepatitis C	1997 US	Amgen
<b>Glucagon</b>	Hypoglycemia	1998 US	Eli Lilly
<b>Beromun (tasonermin)</b>	Soft sarcoma	1999 EU	Boehringer Ingelheim
<b>Ontak (denileukin diftitox)</b>	Cutaneous T-cell lymphoma	1999 US	Seragen Inc.
<b>Lantus (long-acting insulin glargine)</b>	Diabetes	2000 US	Aventis
<b>Kineret (anakinra)</b>	Rheumatoid arthritis	2001 US	Amgen
<b>Natrecor (nesiritide)</b>	Congestive heart failure	2001 US	Scios Inc.

Table 1 continued.

<b>Somavert (pegvisomant)</b>	Acromegaly	2003 US	Pharmacia NV
<b>Calcitonin (recombinant calcitonin salmon)</b>	Post menopausal osteoporosis	2005	Upsher- Smith Laboratories
<b>Lucentis (ranibizumab)</b>	Wet age-related macular degeneration	2006 US	Novartis
<b>Preotact (human parathyroid hormone)</b>	Osteoporosis	2006 EU	Nycomed Danmark
<b>Krystexxa (rh urate oxidase, PEGylated)</b>	Gout	2010	Saviant
<b>Nivestim (filgrastim, rhGCSF)</b>	Neutropenia	2010	Hospira
<b>Voraxaze (glucarpidase)</b>	Lowering of toxic level of methotrexate concentration in patients with impaired renal function	2012	BTG International
<b>Preos (parathyroid hormone)</b>	Osteoporosis, hypoparathyroidism	2013 EU	NPS Pharmaceuticals

*E. coli* remains strong as one of the most desired expression systems for both scientific research usage and protein therapeutics manufacturing. The rapid growth of *E. coli* allows for high production rate and minimal risk of contamination. After decades of research and development, well-structured frameworks and toolboxes are available for *E. coli* recombinant expression, which makes new strain construction relatively easy.

Recombinant protein can be accumulated up to 30% of the total *E. coli* protein which gives a great starting point for extraction and purification<sup>29</sup>.

Although *E. coli* expression system is usually incapable of glycosylation and phosphorylation due to the lack of cellular machinery<sup>31</sup>, recombinant OPN from *E. coli* made major contributions to OPN related research as multiple functions of the protein relies mainly on its primary structure. *E. coli* expressed OPN showed cell adhesion enhancement, cell proliferation activities<sup>32</sup> and, cell migration improvement activities<sup>4</sup>. And full length bioactive OPN without variance introduced by post-translational modification can be a great material for research usage and antibody development. *In vitro* phosphorylation of OPN has been achieved since 1993<sup>33</sup>, which makes producing full-length PTM free OPN an versatile option for phosphorylation related studies of OPN.

### *1.2.3 Protein purification by chromatography*

Chromatography has been the work horse of protein purification in biopharmaceutical industry. The separation power provided by chromatography is unparalleled from other non-chromatographic methods thus essential for injectable biopharmaceuticals for which high purity is an absolute necessity. Chromatography process for biopharmaceuticals often requires high-quality chromatographic medium (resin) for maximum resolution, expensive pumping systems for precise flow controls and highly-skilled labor forces to operate them, which all contribute to the high cost of chromatography processes. In fact, chromatography is one of the major contributors of the overall cost for biopharmaceutical manufacturing and sometimes dictates the

financial feasibility of drug candidates. Therefore, the design and optimization of chromatography steps are vitally important for biopharmaceutical process development, which is exactly what this research is focusing on.

Proteins adsorb to the solid phase by various kinds of physio-chemical interactions such as electrostatic interaction, hydrophobic interaction, and the combination of the two. The specific interactions and their applications are discussed in the following sections.

Chromatography for protein purification often works in either one of the two modes—bind/elute mode and flow-through mode. For bind/elute mode, target protein adsorbs to the stationary phase (ligands on resins in most cases) and gets retained during sample loading while impurities flow through. Then by altering the conditions of the mobile phase, protein-resin interaction can be disrupted allowing the elution of the protein from the column. Multiple steps with different conditions or gradient elution can be used to further fractionate the molecules bound to the column for maximum separation. Bind/elute mode is useful for most protein purification practices especially as the capture step due to its ability for volume reduction. For flow-through mode, loading conditions need to be selected that the target protein would not be retained by the resin while impurities would. The target protein can be collected in the flowthrough fraction with the impurities removed. Flow-through mode chromatography often applied as the polishing step for biopharmaceuticals. For example, anion exchange resins are used to bind and remove negatively charged impurities such as leached protein A and DNA from almost charge neutral antibodies after they are captured by protein A affinity columns.

### 1.2.3.1 Ion exchange chromatography (IEX)

Ion exchange chromatography in protein purification relies on the reversible electrostatic interactions between proteins in the mobile phase and the stationary phase of opposite charge. IEX resins are categorized as anion (negatively charged group) or cation (positively charged group) and can be further categorized as strong or weak. Resin selection usually begins with strong ion exchangers (Q or,S) for their ability to work in broad range of pH conditions. Weak ion exchangers should be considered when the selectivity provided by strong ion exchangers is unsatisfactory.

**Table 2** List of commonly used ion exchangers for protein purification

Type of Ion Exchanger	Common Abbreviation	Functional Group
Strong Anion	Q	Quandary Ammonium
Weak Anion	DEAE	Diethylaminoethyl
Strong Cation	S	Sulfonic Acid
Weak Cation	CM	Carboxymethyl

The resin selection and adsorption condition design is highly dependent on the isoelectric point (pI) of the protein and the pKa of the ligand. Isoelectric point is the pH condition where the net charge of a protein stays neutral. Figure 2 is a visual representation of how protein charge varies under different pH conditions based on ProtCalculator simulation program. OPN has zero charge when at its pI which in this program is predicted to be 4.6 by the algorithm. When the pH in the solution is below the pI, protein takes a positive net charge. When the pH becomes higher than the pI of

protein, protein becomes negatively charged. Therefore, in the case of OPN, anion exchange sorbents could be used for OPN adsorption at pH above 5 and cation exchange sorbents could only be used when pH is below 4, which are the conditions used and reported for OPN purification<sup>4</sup>.

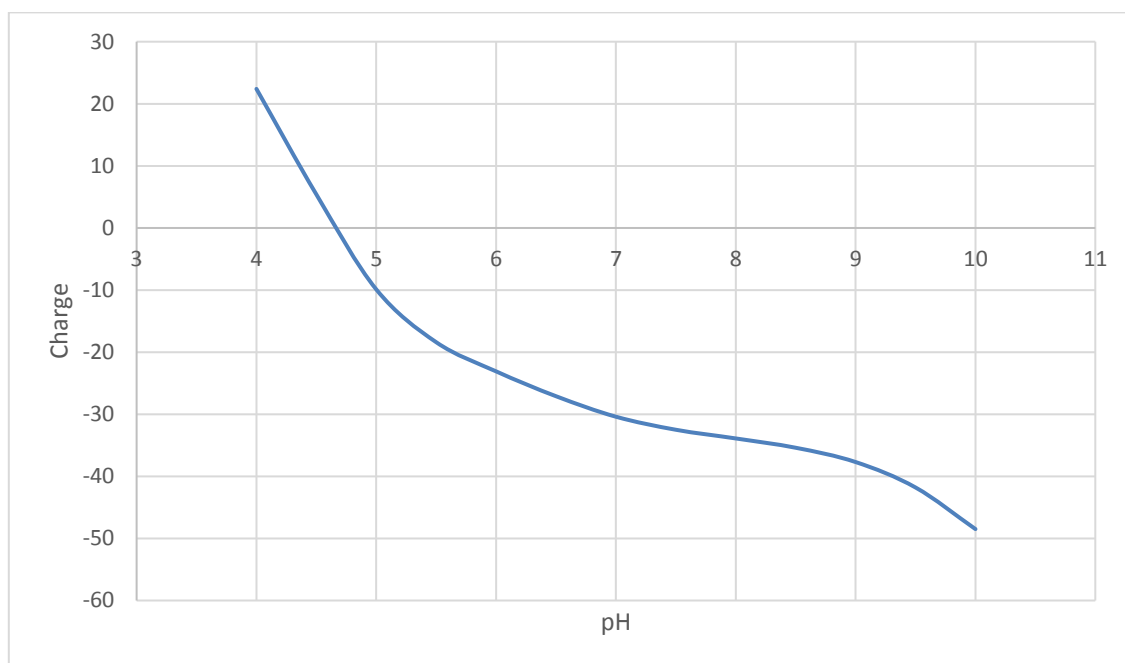


**Figure 2** Surface charge prediction of OPN, plotted from prediction generated by ProtCalculator v3.4 (ProtCalc.net)

For ion exchange chromatography, low ionic strength conditions are often required for efficient adsorption and ascending salt concentration solutions can disrupt the electrostatic interactions between oppositely charged proteins and ligands, so often applied as elution buffer.

### 1.2.3.2 Hydrophobic interaction chromatography (HIC)

Hydrophobic interaction chromatography works by utilizing the reversible interaction between the hydrophobic patches on the protein in the solution and the



hydrophobic surface of the HIC resin. HIC fractionates proteins based on their differences in surface hydrophobicity.

The hydrophobicity of resins varies with ligand structure, ligand density and the backbone structure of the resin. Figure 3 demonstrated HIC resins with different hydrophobicity from the same manufacturer.

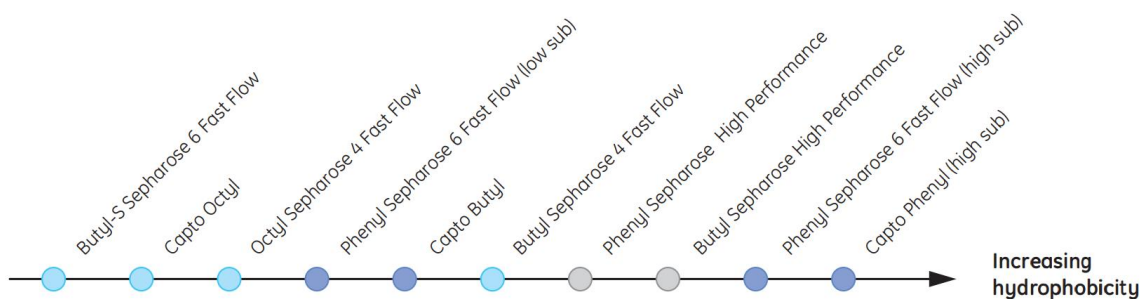


**Figure 3** Hydrophobicity of HIC resins (Reprint from GE Healthcare Lifesciences<sup>34</sup>)

HIC usually requires high ionic strength condition to promote hydrophobic interactions between protein and resin for efficient adsorption. Therefore, HIC can be particularly useful as a capture step after the crude extract was fractionated by salt precipitation or as a polishing step after ion exchange chromatography, since in both cases the samples are already in high salt conditions.

However, high ionic strength conditions also promote hydrophobic interaction between proteins which may result in protein loss due to aggregation. Therefore, one of the most important parameters in HIC process development is determining the maximum salt concentration in which target protein remains stable in the solution. Protein elution can be achieved by decreasing the salt concentration in the elution buffers.

### 1.2.3.3 Mixed-modal chromatography (MMC)

Mixed-modal chromatography sorbents have caught attention from separation developers in recent years for its unique features comparing to traditional single mode chromatography media.

One advantage of mixed-modal chromatography is a wide variety of chemistries that could provide orthogonality to traditional single mode chromatography. For example, Capto adhere resin has been developed and commercially employed to remove antibody aggregates and leached protein A at the same time during monoclonal antibody production<sup>35</sup>. Mixed-modal sorbents have been tested as alternatives to protein A resin for antibody capture<sup>36-39</sup> and capture chromatography step for recombinant proteins from *E.coli* crude extract as well<sup>40-43</sup>. In the latter case, mixed- modal adsorption exhibited unique advantages over single mode sorbents.

Since this study focuses on resins with mixed ionic and hydrophobic properties, key chemistries and properties of mixed-modal ligands is reviewed next. Hydrocarbyl amines are among the popular MMC ligands as the amine group serves as the active sites for immobilization and the positively charged group for electrostatic interaction while the hydrocarbon group provides hydrophobicity to the resin (Table 3)<sup>44</sup>. Protein adsorption to hydrocarbyl amine based resins takes advantage of both ion exchange and hydrophobic properties and elutions are often achieved at low pH when electrostatic repulsion overcomes hydrophobic attraction. Commercialized resins HEA HyperCel and PPA HyperCel tested in this research belong to this category.

Adding phenyl groups and hydrogen bonding groups to traditional ion exchangers gives mixed-modal features to IEX resins. Commercialized examples for such resins are Capto adhere and Capto MMC which are designed this way to be mixed-modal anion exchanger and cation exchanger respectively.

Other type of resins that have hydrophobic and ion exchange properties are designed so that the charge on the ligand varies with the change of pH in the solution. Chromatographic separations with these types of resins are referred to as hydrophobic charge induction chromatography (HCIC). 4-Mercaptoethylpyridine (MEP) resin with a pKa of 4.85 is an example of hydrophobic charge induction chemistry (Table 3). At pH above 4.85, the ligand remains neutral charge and binds protein via hydrophobic interactions. When the pH of the solution drops below ligand pKa and protein pI, the protein is rejected due to electrostatic repulsion.

As described in the previous sections, IEX adsorption often requires low conductivity but HIC adsorption for proteins usually needs high ionic strength conditions. The conflicting ionic strength requirements underscore the fundamental features of mixed-modal resins, which makes optimal conditions for protein adsorption hard to predict. This is why high-throughput screening (HTS) is helpful allowing testing wide range of pH and conductivity conditions in parallel for comprehensive understanding of protein and mixed-modal interactions<sup>42, 45-46</sup>. Because specific interactions of both the target protein and host cell proteins (HCPs) with a selected resin dictates the separation efficiency, HTS technology becomes a particularly helpful tool

for identifying optimal pH and ionic strength conditions i.e. “the sweet spot” for target protein purification.

**Table 3** List of mixed-modal chromatography resins (Reprint from Zhao et al. 2009<sup>47</sup>)

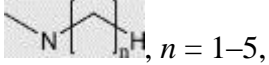
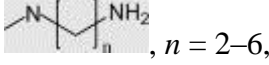
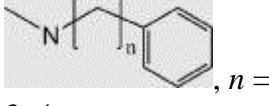
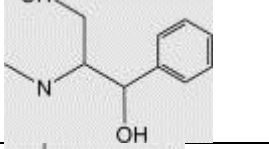
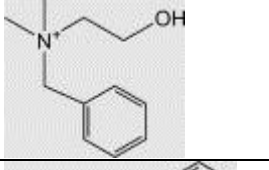
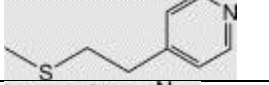
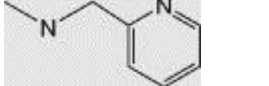
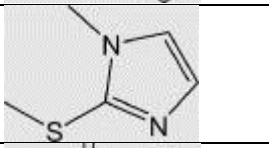
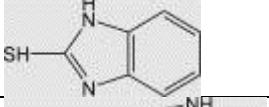
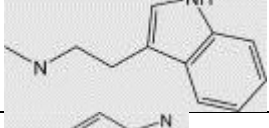
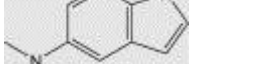
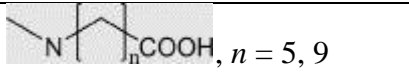
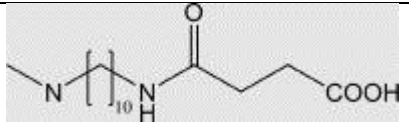
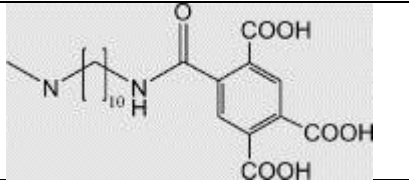
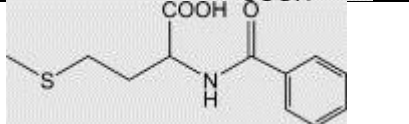
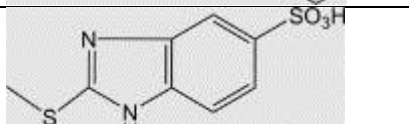
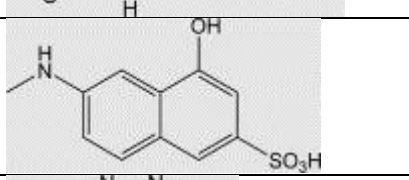
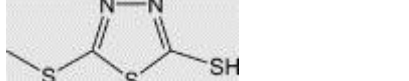
	Name	Structure	pKa
Ligands with positive charge	Alkylamine	 $n = 1-5,$ 6, 8	≈10
	α,ω-Diamino alkane	 $n = 2-6, 8,$ 10	≈10
	Phenylalkylamine	 $n = 1,$ 3, 4	6-7
	2-Amino-1-phenyl-1,3-propanediol		9.0
	N-Benzyl-N-methyl ethanol amine <sup>c</sup>		–
	4-Mercaptoethylpyridine		4.85
	2-Aminomethylpyridine		pKa <sub>1</sub> = 2.2, pKa <sub>2</sub> = 8.5
	Mercaptomethylimidazole		5.3
	2-Mercaptobenzimidazole		4.1
	Tryptamine		10.3
5-Aminoindole		3.9	

Table 3 continued.

Ligands with negative charge	Aminoalkyl carboxyl acid		5.2
	N-(3-Carboxypropionyl) aminodecyl amine		9.1
	N-pyromellityl aminodecyl amine		pKa <sub>1</sub> = 2.2, pKa <sub>2</sub> = 3.4, pKa <sub>3</sub> = 5.4,
	2-Benzamido-4-mercaptobutanoic acid		3.3
	2-Mercapto-5-benzimidazole sulfonic acid		–
	6-Amino-4-hydroxy-2-naphtalene sulfonic acid		–
	2,5-Dimercapto-1,3,4-thiadiazole		6.3

#### 1.2.4 OPN purification methods

Different approaches to produce purified OPN for biochemistry studies have been reported. Milk is one of the most used source to recover OPN. Anion exchange chromatography has been the default capture step for OPN recovery since the 1989<sup>3</sup>.

In addition to precipitation steps for lipids and casein removal, multiple chromatography steps are often applied to purify OPN from milk. Bayless and colleagues used weak ion exchanger DEAE to capture OPN from skim milk. It took them two additional HIC steps to obtain purified OPN. Both HIC steps involved Phenyl-

Sepharose resin and 2 M NaCl as the elution condition. The only difference between the two consecutive HIC steps was the binding conditions which were 4 M and 5 M NaCl respectively. The first HIC step could only elevate purity to 35% and the purity finally reached close to 100% after the second HIC<sup>5</sup>. The use of similar steps in series is never ideal in terms of economic feasibility. Sørensen et al. went for direct capture by anion exchange chromatography from milk before casein removal. Hydroxyapatite chromatography with sodium phosphate elution and negative affinity chromatography were added to the process to purify OPN from other milk protein<sup>48</sup>. However, the negative affinity chromatography used in this process is not applicable for large scale production. Azuma et al. used DEAE based anion exchange chromatography at pH 5 taking advantage of the low pI of OPN to purify OPN from milk to 85% in one step. Another anion exchange chromatography step was used to remove residual milk protein to obtain purified OPN in the process<sup>49</sup>. However, none of the processes reported overall yield due to the fact that the concentration of OPN in raw milk were below their detection limits. Moreover, molecular weight variation due to different degree of modification was observed from OPN purified from milk.

Various strategies have been applied to purify OPN from recombinant *E. coli*. Fusion tags were widely used for OPN biochemistry researches since the early days for its convenience in purification. Glutathione S-transferase (GST) affinity chromatography was among the most popular for OPN and yielded highly purified OPN in a single step due to the high specificity provided by strong affinity between GST and glutathione.<sup>50-51</sup> His-tag was also used in the construct of recombinant OPN in *E. coli*.<sup>32</sup> However, these

methods were used to produce micrograms of purified OPN for biochemistry studies without supporting evidence of yield and potential scalability. Large tags such as GST require removal steps which add expenses. Since there is a thrombin cleavage site near the RGD domain in the OPN sequence, thrombin would destroy the RGD-mediated adhesion activities of OPN. Thrombin cleavage being a popular method for large tag removal is not an option used in full-length OPN production, which adds difficulties in using tags for OPN purification<sup>51</sup>. In general, tagged proteins are not desirable for injectable therapeutics.

Non-tag methods for OPN purification from recombinant *E. coli* were also reported. Based on OPN's calcium binding nature, hydroxyapatite chromatography was used as the single chromatography step to purify OPN from *E. coli* lysate. The feed of hydroxyapatite chromatography was fractionated by ammonium sulfate precipitation and recovered from 20% to 40% ammonium sulfate precipitates. However, this process was done at the microgram scale and no evidence of purity nor recovery was reported<sup>52</sup>. A series of precipitation steps (isoelectric precipitation steps at pH 6, 5, 4.3 and the supernatant was precipitated by 20% saturation ammonium sulfate and then re-solubilized) achieved 45% OPN purity from 7% purity *E. coli* lysate, while yield dropped to 21% during the precipitation steps. A final purity of 97% was achieved by additional two ion exchange chromatography steps with conditioning steps in between. The overall yield was as low as 12.8%<sup>4</sup>. In general usage of multiple precipitation and non-orthogonal processes in series are not ideal in downstream processing, yet there are no other strategies that have higher efficiency for OPN recovery to date. The lack of

high yield and high efficiency strategies for OPN production hindered related research from moving on to larger scale.



## 2 MATERIALS AND METHODS

### 2.1 *E. coli* cell cultivation and harvest

The OPN recombinant *E. coli* strain is provided by collaborator from University of California, San Diego. The construct was based on BL21-AI strain. The production of recombinant OPN was regulated by arabinose inducible promoter. A FLAG fusion tag was added to the N-terminus of recombinant OPN for detection and identification. The strain construct contains an ampicillin resistance selective marker.

The strain was kept as frozen stock cell bank in 25% glycerol at -80°C for long term storage.

To start new culture, 1 mL of frozen stock cell was inoculated in 25 ml Miller's Luria Broth (LB medium, Miller's) (Sigma-Aldrich, L3522) with 150 µg/ml ampicillin (Sigma-Aldrich, A1593) and incubated at 37°C on an orbital shaker at 200 rpm for 5 hours. 5 ml of seed culture was transferred to 500 ml Terrific Broth (Sigma-Aldrich, T0918) with 50 µg/ml ampicillin and incubated at 37°C and 200 rpm shaking until OD<sub>600</sub> reached 0.8. The recombinant protein production was induced by adding arabinose (Sigma-Aldrich, A3256) to a final concentration of 0.2% (w/v). And the cells were incubated at 37°C with 200 rpm mixing overnight. The cells were harvested by centrifugation at 3,000 g for 10 minutes at 4°C. The harvested cell biomass was kept in -80°C until use.

### 2.2 Cell lysis and protein extraction

The frozen biomass was suspended in lysis buffer (50 mM Tris, 150 mM NaCl, 1 mM PMSF, pH 7.4) at 1:10 (w/v) ratio in room temperature. The suspended cells then

were lysed by sonication (QSonica, Q55) with 30 seconds on and 30 seconds off cycle on an ice bath for 5 cycles at 40% amplitude. The cell debris was removed by centrifugation at 15,000 g for 30 minutes at 4°C. The supernatant was collected and filtered with a 0.22 µm syringe filter (PES membrane, Olympus plastics) to produce clarified cell lysate, which was the starting material for all experiments discussed in this thesis.

### **2.3 High-throughput screening (HTS) of mixed-modal sorbents**

HTS experiments were performed to study the interaction between OPN and various mixed-modal ligands at varying NaCl and pH conditions. Salt concentration and pH were tested at multiple levels using full factorial design experiments with 3 replicates. A 3x3 full factorial design (pH 5, 7, 9 and NaCl concentration 0, 1.5, 3 M) was performed for HEA HyperCel and PPA HyperCel resins. For Capto adhere, 4x3 full factorial design (pH 5, 6, 7, 8 and NaCl concentration 0, 0.4, 0.8 M) was used. The pH of cell lysate was adjusted with 0.2 M HCl or 0.2 M NaOH. The salt concentration was adjusted by adding solid NaCl to the cell lysates to the designed concentration or by dialysis when salt removal was required. The pH and/or salt adjustment was followed by end-over-end mixing for 15 minutes and clarification by centrifugation at 15,000 g for 30 minutes at 4°C to remove any protein precipitates that might have formed during condition adjustment. The resulting samples were referred to as conditioned lysate and served as starting feed for HTS experiments.

Adsorption experiments were carried out by dispensing 0.05 mL of resin (supplied as 50% slurry) in a 96-well filter plate (3M Empore). The resin storage buffer

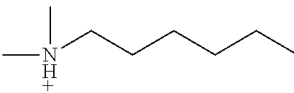
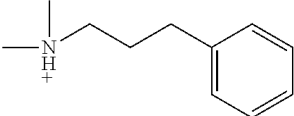
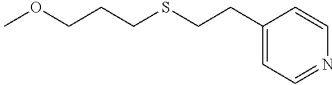
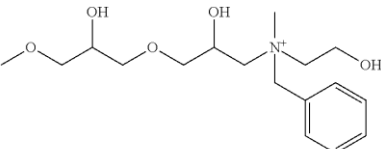
was removed by centrifugation at 300 g for 7 minutes at 4°C. Resin equilibration was achieved by adding 0.2 mL (4 resin column volumes) of prescribed loading buffer to each resin in the wells. The resin and loading buffer in the wells were mixed gently for 10 minutes. After that the buffer was removed by centrifugation at 300 g for 7 minutes. The resin equilibration process was repeated twice. Conditioned lysate (0.2 mL of lysate for each well) was then added to the equilibrated resin and incubated with gentle mixing for 1 hour at room temperature. The unbound sample was collected by centrifugation (300 g, 7 minutes, 4°C) for analysis. Total protein of the samples was measured by Bradford assay and OPN concentration by ELISA. The procedure was repeated for each of the tested resins, HEA HyperCel, PPA HyperCel and Capto adhere.

#### **2.4 Batch adsorption and elution of OPN**

Batch adsorption experiments followed by gravity-flow elution were used as a scale-down model for optimizing bind/elute conditions and resin performance evaluation. The chromatography adsorbents (resins) screened in this study included strong anion exchanger Capto Q, traditional hydrophobic interaction resin Phenyl Sepharose (6 Fast Flow, high sub), and 5 mixed-modal sorbents— HEA HyperCel, PPA HyperCel, MEP HyperCel, Capto adhere, and ceramic hydroxyapatite (CHT).

Capto Q, Phenyl Sepharose and Capto adhere were purchased from GE Healthcare, HEA, PPA and MEP HyperCel from Pall, and Ceramic Hydroxyapatite from Bio-Rad. The ligand structure and primary adsorption chemistry are listed in Table 4.

**Table 4 List of candidate chromatography sorbents for OPN purification.**

Adsorbent (Resin)	Vendor	Adsorption chemistry	Ligand structure	Matrix
HEA HyperCel	Pall	Hydrophobic interaction; Electrostatic interaction	Hexylamine 	Cellulose
PPA HyperCel	Pall	Hydrophobic interaction; Electrostatic interaction	Phenylpropylamine 	Cellulose
MEP HyperCel	Pall	Hydrophobic interaction	4-Mercaptoethylpyridine 	Cellulose
Capto adhere	GE	Electrostatic interaction; Hydrophobic Interaction	N-benzyl-n-methyl ethanolamine 	Agarose matrix with dextran surface extender
Ceramic hydroxyapatite	Bio-Rad	Calcium affinity; Electrostatic interaction	(Ca <sub>5</sub> (PO <sub>4</sub> ) <sub>3</sub> OH) <sub>2</sub> matrix serves as both backbone and ligand	
Capto Q	GE	Electrostatic interaction	Quaternary amine	Agarose matrix with dextran surface extender
Phenyl Sepharose (6 Fast Flow, high sub)	GE	Hydrophobic interaction	Phenyl	Spherical 6% cross-linked agarose

The general batch adsorption experiment procedure with all candidate resins was as follows: Conditioned cell lysates were incubated with pre-equilibrated sorbents for 1 hour with end-over-end mixing at room temperature. The loading volume was set at 6 column volumes (1.2 ml conditioned lysate load to 0.2 ml resin) for all the resins tested, equivalent to feeding about 30 mg total protein/ml resin. The lysate-resin mixture was then loaded on a PolyPrep column (Bio-Rad) and the unbound protein after equilibrium binding would pass through and be collected by gravity as “Flowthrough”. The resin was washed with 10 column volumes of loading buffer. Adsorbed proteins were eluted using 10 column volumes of appropriate elution buffer. All the samples were collected by gravity for analysis. The average gravity-driven linear velocity during elution was about 100 cm/h. The specific protocols designed for individual resins are listed below:

Capto Q batch adsorption and elution. The clarified lysate was conditioned by dialysis against 50 mM Tris buffer (pH 7) overnight at 4°C for salt removal using SnakeSkin dialysis tubing (MWCO = 3.5 kDa, ThermoFisher Scientific). The conditioned lysate was incubated with Capto Q resin for 1 hour at room temperature by end-over-end mixing. The lysate-resin mixture was then transferred to PolyPrep column (Bio-Rad) and the “flowthrough” sample was collected by gravity. The resin was washed by 20 column volume of 50 mM Tris pH 7 binding buffer. The elution was achieved in 3 stages: 0.2 M NaCl, 0.5 M NaCl, and 1 M NaCl. All elution buffers were buffered by 50 mM Tris at pH 7.

Phenyl Sepharose batch adsorption and elution. The clarified lysate was conditioned by adding solid ammonia sulfate to 1 M, mixing end-over-end for 15

minutes and clarified by centrifugation at 15,000 g for 30 minutes. The conditioned lysate was applied to Phenyl Sepharose FF high sub resin which was pre-equilibrated by binding buffer (50 mM Tris pH 7 buffer with 1 M ammonia sulfate). Conditioned lysate and resin were incubated for 1 hour at room temperature before being loaded onto PolyPrep column. When the unbound sample flew through, 20 CV binding buffer were added on top of the gravity packed column to wash out the residual unbound proteins. Protein elution from Phenyl Sepharose was done in 2 stages: 0.5 M ammonia sulfate and 0 M ammonia sulfate. Both elution solutions were buffered by 50 mM Tris at pH 7.

Ceramic Hydroxyapatite (CHT) batch adsorption and elution. The clarified lysate went through overnight dialysis against pH 6.8, 5 mM sodium phosphate (NaP) buffer at 4°C using SnakeSkin dialysis tubing (MWCO = 3.5 kDa, ThermoFisher Scientific). The conditioned lysate was then incubated with pre-equilibrated CHT resins (Type I, 80 µm) for 1 hour at room temperature with end-over-end mixing. Then, the lysate-resin mixture was loaded to PolyPrep column and the unbound fluids flew through the column to be collected as “flowthrough”. After the resin was washed by 20 CV of binding buffer (5 mM NaP pH 6.8), the elution process was carried out by step-wise ascending NaP concentration buffers. The first elution buffer was 0.1 M NaP pH 6.8 buffer and the second one was 0.2 M NaP both at pH 6.8.

HEA HyperCel low salt batch adsorption and elution. HEA HyperCel low salt binding condition was the same as the lysate condition (150 mM NaCl, 50 mM Tris, pH 7). Therefore, no additional conditioning step was required. The clarified lysate was directly incubated with HEA HyperCel resin for 1 hour at room temperature which was

pre-equilibrated with binding buffer (50 mM Tris, pH 7 buffer with 150 mM NaCl). The lysate-resin mixture was then transferred into a PolyPrep Column and the flowthrough sample was collected by gravity. The resin then was washed by 20 CV binding buffer and the wash sample was also collected for further analysis. Protein elution was designed to be a 3-step process with 10 CV of each elution buffer. The first elution was achieved by 1 M NaCl, 50 mM Tris pH 7 buffer. The second elution was pH 5 100 mM sodium acetate (NaAc) buffer also with 1 M NaCl. The third elution buffer was pH 3 100mM sodium citrate buffer with no NaCl addition.

HEA HyperCel high salt batch adsorption and elution. Another binding condition tested for HEA HyperCel resin was at high salt concentration. Solid NaCl was added into clarified lysate to reach a final NaCl concentration of 3 M. After 15 minutes of end-over-end mixing, the lysate was centrifuged at 15,000 g for 30 minutes to remove any precipitates that formed. The conditioned lysate was then incubated for 1 hour at room temperature with pre-equilibrate HEA HyperCel resin by the high salt binding buffer (50 mM Tris, pH 7, 3 M NaCl). The lysate-resin mixture was then transferred into a PolyPrep Column and the flowthrough sample was collected by gravity. The wash and elution procedure following HEA high salt batch adsorption was exactly the same as HEA low salt batch adsorption.

PPA HyperCel low salt batch adsorption and elution. The PPA low salt batch adsorption and elution experiment followed the same protocol as HEA low salt batch adsorption and elution experiment.

PPA HyperCel high salt batch adsorption and elution. Similarly, the PPA low salt batch adsorption and elution experiment followed the same protocol as HEA high salt batch adsorption and elution experiment.

Capto adhere batch adsorption and elution. For Capto adhere adsorption, the same adsorption conditions and lysate conditioning steps as Capto Q adsorption were applied. The Elution process for Capto adhere was different from Capto Q to achieve the optimal purification power for Capto adhere. Elution was designed to have 3 stages of descending pH change (pH 5, 4, and 3). All elution buffers were 0.1 M citrate-phosphate buffer with no extra salt addition.

MEP HyperCel batch adsorption and elution. MEP HyperCel batch adsorption and elution used the same procedure as the high salt conditions as HEA and PPA HyperCel.

## **2.5 Packed-bed purification of OPN**

ÄKTA Purifier (GE healthcare life sciences) carried packed-bed chromatography purification and process optimization. The top two resin performers from batch adsorption experiments were evaluated in a 1 mL prepacked column format. PRC HEA HyperCel (1 ml) was purchased from Pall and HiTrap Capto Q (1 ml) from GE Healthcare. The same feed composition and load volume was used on prepacked columns to allow for verification and comparison between batch adsorption and packed-bed chromatography data.

The general protocols for packed-bed chromatography in this research are as follow. The volumetric flow rate was controlled at 0.2 ml/min to ensure 5 minutes



residence time during sample loading. The same linear velocity was used for the wash and elution steps. Protein concentration during chromatography and ionic strength of elution buffers was by monitored continually by absorbance reading at 280 nm and conductivity measurement, respectively. Eluted fractions (1 ml) were collected in fraction collector (Frac-950, GE healthcare life sciences) and analyzed for total protein by Bradford assay and OPN by ELISA. The elution process was the subject to change and optimization on packed-bed chromatography.

HEA HyperCel resin performance verification and optimization. To verify performance of HEA HyperCel from batch adsorption experiments on packed-bed columns and further optimize the purification process, clarified lysate (in pH 7 50 mM Tris buffer containing 150 mM NaCl) was loaded onto the equilibrated PRC HEA HyperCel column and washed by 20 CV of binding buffer. Linear NaCl gradient (0.15 to 1.5 M NaCl over 20 CV) in 50 mM Tris at pH 7 was applied as the elution process.

Capto Q resin performance verification and optimization. To verify performance of Capto Q on packed-bed columns and optimize the purification process, clarified lysate was dialyzed against pH 7 50 mM Tris buffer overnight to bring conductivity below 5 mS. Then loaded onto the equilibrated HiTrap Capto Q column. After washing by 20 CV of binding buffer, linear NaCl gradient (0 to 1.0 M over 20 CV) in 50 mM Tris at pH 7 was applied to elute bound proteins:

OPN purification by HEA-Q 2-step process. Clarified lysate (in pH 7 50 mM Tris buffer containing 150 mM NaCl) was directly loaded onto the equilibrated PRC HEA HyperCel column and washed by 20 CV of binding buffer. A single step change

elution was used for OPN recovery from HEA. The elution buffer was 50 mM Tris pH 7 buffer containing 1 M NaCl. The first 8 CV of elution fraction was collected as the HEA purified pool. The partially purified OPN from HEA HyperCel elute was dialyzed against 50 mM Tris pH 7 buffer overnight at 4°C for salt removal. Dialyzed HEA eluate (conductivity <5 mS), was loaded on HiTrap Capto Q (1 ml) as previous protocols, washed with 20 column volumes of the binding buffer (50 mM Tris, pH 7, 4 mS). After the wash procedure, 0 – 1 M NaCl linear gradient elution (20 CV) was applied to Capto Q for OPN purification.

OPN purification by Q-HEA 2-step process. The process for Capto Q as capture chromatography step was the same as its performance verification and optimization. The fractions between 32 mS/cm and 49 mS/cm were collected as the partially purified OPN pool. The pool was then diluted by 50 mM Tris pH 7 buffer 3 times to reduce the conductivity for HEA HyperCel low-salt binding. The binding, washing and eluting for HEA HyperCel was actually the same as the process. Then, HEA was used as the capture step. The elute from HEA was collected as the purified OPN by Q-HEA 2-step process.

## **2.6 Analytical methods**

### *2.6.1 Bradford assay for total protein (TP) determination*

The total protein concentration in clarified cell lysate and fractions collected in all the experiments was determined by Bradford assay<sup>53</sup> in 96-well plates with bovine serum albumin (BSA) standards (Pierce™ Coomassie Plus (Bradford) Assay Kit, ThermoFisher Scientific).

The protein concentration standards were made by diluting 2 mg/ml BSA stock solution included in the kit in PBS to concentration 1500, 1000, 750, 500, 250, 125, 100, and 25 µg/ml. The samples for total protein quantification were diluted in PBS if out of the range of standard curve. Samples and standards were dispensed in 96-well plate in triplicates and mixed with Coomassie Plus Blue stain from the kit and incubated in room temperature for 10 minutes. The absorbance was read at 595 nm wavelength by VERSA max microplate reader (Molecular Devices, Sunnyvale, CA, USA).

#### *2.6.2 ELISA (enzyme-linked immunosorbent assay) for OPN quantification*

The standards were prepared from FLAG-BAP (Sigma-Aldrich P7582) diluted in PBS to concentration standards ranging from 15 ng/ml to 1000 ng/ml. The samples were also diluted in PBS to match the range of the standard curve. Standards and diluted samples were dispensed in 96-well plate (Nunc Maxisorp immuno plate, Thermo Fisher) at 100 µl/well and incubated at 4°C overnight. After blocking by 3% BSA, the FLAG tagged protein were detected by 1:5000 diluted anti-FLAG M2 antibody conjugated with Horseradish peroxidase enzyme (HRP) (Sigma-Aldrich A8592). The plate then was developed for 5 minutes by the addition of TMB liquid substrate (Sigma-Aldrich T0440) and then the reaction was ended by adding 2 N HCl. The absorbance was read at 450 nm.

#### *2.6.3 SDS- PAGE and Western- blot for product quality measurement*

The purified fractions along the process were analyzed by SDS-PAGE (Sodium dodecyl sulfate-polyacrylamide gel electrophoresis) for OPN purity. The samples were mixed with sample buffer (NuPAGE LDS Sample buffer 4x, ThermoFisher scientific)

which contains 10% reducing agent and heated to 70°C for 10 min. The reduced sample then were loaded onto the NuPAGE 4-12% Bis-Tris Gel (Invitrogen, USA) and the electrophoresis was carried out at 200 V for 35 minutes. Next, gels were removed from the cassette, blocked 45 min in the blocking buffer (10% acetic acid, 40% ethanol, and 50% RO water), stain for 3 hours by SimpleBlue™ Safe Stain (Novex, ThermoFisher Scientific) and then destained overnight in RO water overnight.

For Western-blotting, the protein was transferred to PVDF membrane (Invitrogen iBlot Gel Transfer Stacks, PVDF, mini). The membrane was then blocked by 3% non-fat milk for 1 hour. The immobilized protein was detected by 1:2000 diluted anti-FLAG M2 antibody conjugated with alkaline phosphatase (Sigma- Aldrich A9469).

## 2.7 Resin performance evaluation

The OPN capture performances of candidates resins were evaluated by two major parameters—purification factor and OPN recovery. The fractions collected from batch adsorption and elution experiments were analyzed by Bradford assay for total protein concentration and ELISA for OPN concentration. The purity of clarified lysate and fractions from batch adsorption and elution experiments were calculated by the equation below.

$$Purity = \frac{OPN \left(\frac{mg}{ml}\right)}{TP \left(\frac{mg}{ml}\right)} \times 100\%$$

The recovery of each candidate resin was calculated by dividing the amount of OPN (mg) from the elution fraction with the majority of OPN by the amount of OPN from the conditioned cell lysate (feed).

$$\text{Recovery} = \frac{\text{OPN (mg) in the OPN elution fraction}}{\text{OPN (mg) in the feed}} \times 100\%$$

Purification factor of each candidate resin was defined as the ratio of purity of the elution fraction with the majority of OPN and the purity of the feed.

$$\text{Purification factor} = \frac{\text{Purity of the OPN elution fraction}}{\text{Purity of the feed}} \times 100\%$$

## 2.8 Statistical analysis

The statistical analysis used in this article was performed by JMP software.

### 2.8.1 Response surface analysis for HTS results

HTS experiments were used to analyze the response of protein-ligand interaction to different conditions. The OPN and TP bound to the resin after equilibrium binding in the 96-well plate was the difference between the feed and the flowthrough. The fraction of OPN and TP bound to the resin was normalized against the protein concentration in the feed. Response surface analysis was applied to the fraction of the bound OPN and TP with pH and NaCl concentration being the factors. Prediction contour profiles of OPN and TP adsorption were generated based on response surface analysis results.

### 2.8.2 Least square fitting for resin comparison

After OPN purification factor and recovery data was collected by batch adsorption and elution experiments, least square fitting model from JMP Pro software was used to evaluate and compare the performance of different resins.

The first step was to test if different resin yielded significantly different OPN purification performance. The responses in this statistical analysis were OPN recovery

and purification factor. The type of resins was the factor to test. The factor levels were the different resins investigated in this study. For HEA HyperCel and PPA HyperCel resins, two bind/elute processes (low-salt and high-salt process) were investigated using batch adsorption experiments. Each low- and high-salt process conditions were analyzed as individual levels. As a result, a total of 9 levels were tested: Capto Q, Capto adhere, CHT, Phenyl Sepharose, HEA HyperCel (low-salt), HEA HyperCel (high-salt), PPA HyperCel (low-salt), PPA HyperCel (high-salt) and MEP HyperCel. Since the batch adsorption experiments were carried out on multiple days with freshly extracted lysate, the date of experiments was treated as a randomized factor to block the variation associated with the date of experiment and help isolate the effect due to type of resins. Least square fitting analysis was carried out assuming constant standard error. The report included the P-value of fixed factor on the responses as well as the effect of randomized factor. A P-value of less than 0.05 indicated that tested resins had a significantly different performance in terms of OPN recovery and purification.

Once the difference in performance was confirmed, the second step was to identify the better performers among the candidate resins. Each Pair Student's test was conducted to compare the effects between resins based on the least square means generated by the test described in the previous paragraph at  $\alpha = 0.05$  level. The test results with different letters indicate significantly different effect on the response. The connecting letter reports were used to rank and compare resin performance.

## 3 RESULTS AND DISCUSSION

### 3.1 Resin adsorption and elution studies

The low expression level (1.2 mg/g wet biomass) and initial OPN concentration in *E. coli* lysate of 2-3% total soluble protein is a process development challenge for any group that aims to come up with efficient and scalable purification processes. The typical goal for early stage process development is to achieve higher than 90% target protein purity in no more than three chromatographic steps. The overall process yield is difficult to set in advance, but 80% yield per step was a target that we set for OPN purification.

The first step for designing an efficient protein purification process is to screen candidate chromatography media (resins), evaluate their performance, and identify the best performers for further optimization. In the search of efficient adsorbents for OPN purification, we first evaluated most common orthogonal chemistries i.e. anion exchange and hydrophobic interaction resins.

#### 3.1.1 OPN adsorption and elution studies with anion exchange resin (Capto Q)

The relatively low isoelectric point of OPN (4.3) allows strong electrostatic interaction between OPN and the anion exchange resins in a wide range of pH conditions. Preliminary adsorption data using clarified *E. coli* lysates indicated that OPN binds efficiently in the pH range between 6 and 8. However, at pH 8, significantly more *E. coli* host cell protein (HCP) bound to the adsorbent compared to pH 6 and 7. Because pH 7 is the condition of OPN extraction, this condition was chosen for further evaluation of OPN interaction with Capto Q – a strong anion exchange resin.

Clarified and conditioned OPN recombinant *E. coli* lysates (50 mM Tris, pH 7.0, <4 mS) were incubated with Capto Q resin for 1 h at room temperature as described in Materials and Methods. After washing the resin with binding buffer, OPN was eluted stepwise from the resin using 0.2 M, 0.5 M, and 1 M NaCl solution also buffered by 50 mM Tris at pH 7. Total protein (TP) and OPN analysis of each fraction were plotted in Figure 4. The flowthrough sample contained 31% of unbound *E. coli* protein and less than 5% of OPN unbound. The first elution step (0.2 M NaCl) removed the bulk of adsorbed host cell protein (44% of the total protein in the feed) with about 2% loss of OPN. The second elution step eluted almost all of the bound OPN (92%) and the residual total protein (16%). Since the initial feed contained 4 mg/mL TP and 0.16 mg/mL OPN, we can conclude that this two-step elution could achieve a six- fold increase in OPN purity (from 4% to 23%) and 92% OPN recovery. From the standpoint of mass balance, this NaCl concentration step elution could recover 98% of OPN bound to Capto Q as well as 91% of *E. coli* total protein initially bound to the resin.



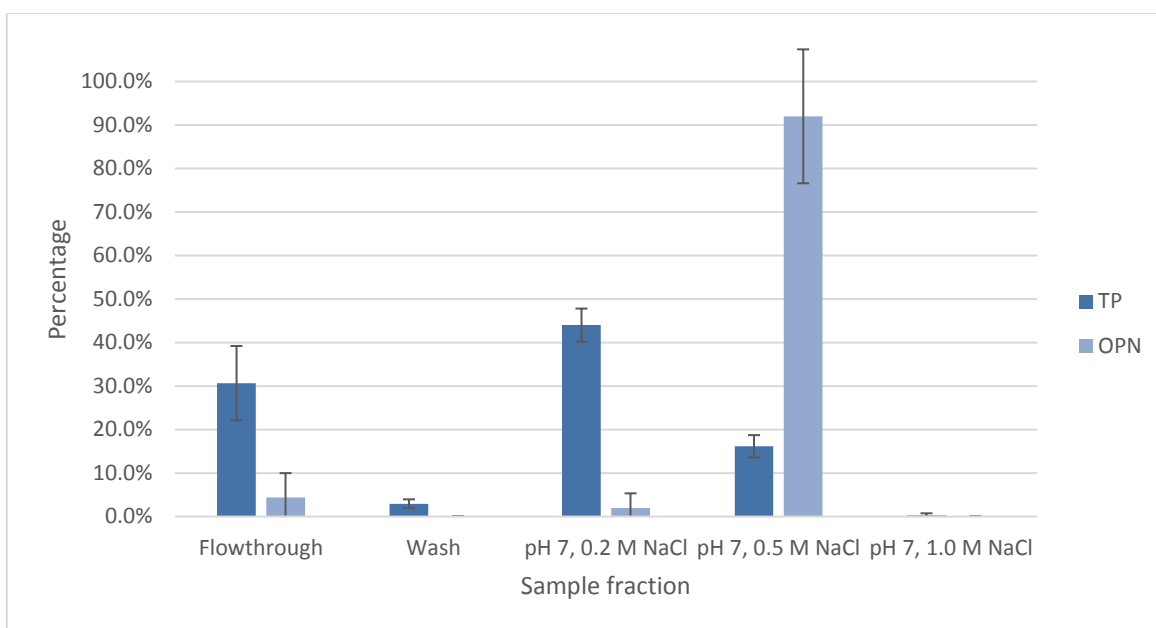


**Figure 4** Batch adsorption and elution of OPN and total protein (TP) on anion exchange resin (Capto Q). Adsorption condition was 50 mM Tris buffer at pH 7. Elution steps were conducted with 50 mM Tris, pH 7 containing 0.2 M, 0.5 M, and 1 M NaCl, respectively. The data reported were percentage normalized against the amount in the feed. The adsorption experiments were performed in triplicate and bars represent the standard deviation.

### 3.1.2 OPN adsorption and elution studies with a hydrophobic interaction resin (Phenyl Sepharose)

Hydrophobic interaction chromatography (HIC) is often applied as an orthogonal step to ion exchange chromatography and in some situations as a capture step of properly adjusted lysates (feed) with ammonium sulfate. To determine maximum ammonium sulfate concentration that can be applied to adjust clarified *E. coli* lysates for optimal OPN binding to Phenyl Sepharose, 1.0 and 1.5 M ammonium sulfate concentrations were tested. The presence of ammonium sulfate in pH 7 lysates at final concentration of 1.0 M or 1.5 M resulted in partial precipitation of OPN and host cell

proteins (HCP) (Table 5). After removing the precipitated protein by centrifugation, we determined that about 20% OPN was lost with 1.0 M and 37% in the presence of 1.5 M ammonium sulfate. The amount of total proteins was reduced by 19% and 28%, respectively. Although, 1.5 M provided a better adsorption of OPN from the lysate, 37% initial loss of OPN was far from ideal. Because no gain of OPN enrichment factor was achieved to counter balance the loss, we decided to test OPN adsorption from clarified lysates containing 1.0 M ammonium sulfate.

**Table 5** Effect of ammonium sulfate addition to *E. coli* lysate on OPN and TP loss due to precipitation. The pellets formed by ammonium sulfate precipitation were removed by centrifugation. OPN and TP recovery in the supernatant and enrichment factors of ammonium sulfate were listed. (The experiments were done in triplicates; data shown with the standard deviation)

<b>Ammonium Sulfate Concentration</b>	<b>OPN Recovery</b>	<b>TP Recovery</b>	<b>Enrichment Factor</b>
1.0 M	79.8% ± 4.6%	88.9% ± 1.7%	0.90 ± 0.06
1.5 M	62.8% ± 4.0%	84.3% ± 2.1%	0.75 ± 0.07

About 20% OPN was lost in the flowthrough and wash fractions after equilibrium binding with 1.0 M ammonium sulfate. Two steps of descending ammonium sulfate concentration (0.5 M and 0 M) were used for the elution of adsorbed protein. About 71% of OPN was recovered by 0.5 M ammonium sulfate elution and a purification factor of 2.9 was achieved. The second elution step with no ammonium sulfate desorbed the rest of OPN bound with no increase in OPN purity (Figure 5).

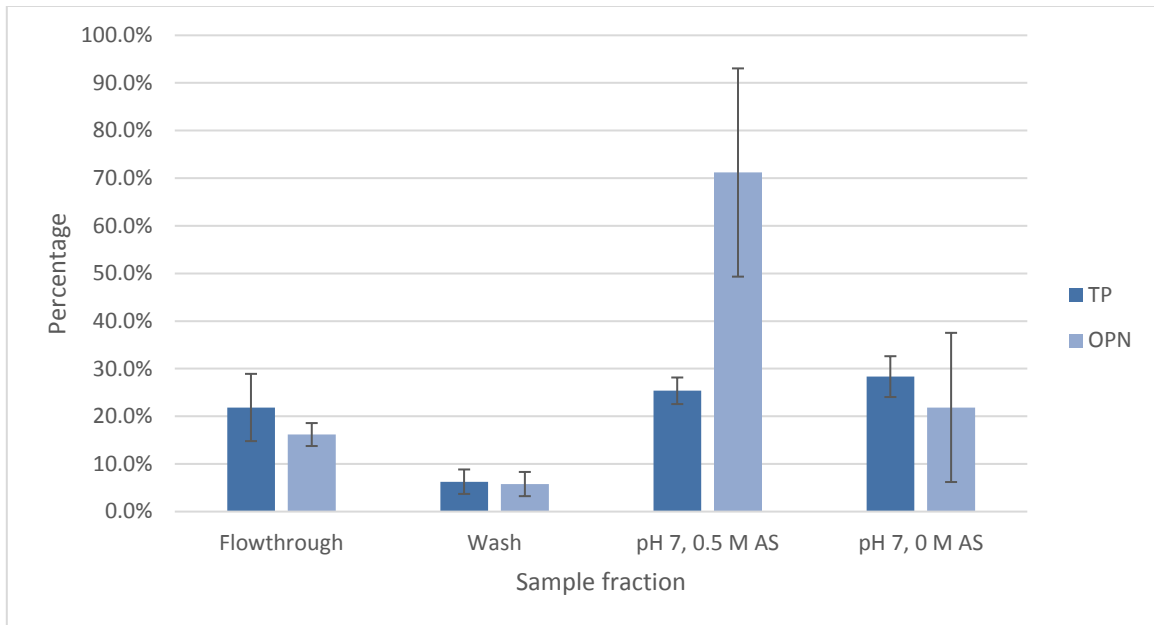


**Figure 5** Batch adsorption and elution of OPN and *E. coli* total proteins by HIC (Phenyl Sepharose). Adsorption was done from conditioned *E. coli* lysate which contained 1.0 M ammonium sulfate at pH 7. Elution steps were 0.5 M ammonium sulfate and 0 M ammonium sulfate. All solutions in this experiment were buffered by 50 mM Tris at pH 7. The data reported were percentage normalized against the amount in the feed. The adsorption experiments were performed in triplicate. Bars represent the standard deviation.

### 3.1.3 OPN adsorption and elution studies with ceramic hydroxyapatite (CHT)

Since binding to calcium is one of the important and differentiating characteristics of OPN, ceramic hydroxyapatite (CHT) were considered a good candidate to test OPN adsorption from cell lysate. The binding and elution conditions with CHT were chosen based on vendor's recommendations that were slightly modified for OPN purification.

CHT showed adsorption preferences for OPN from clarified *E. coli* lysate dialyzed against 5 mM sodium phosphate at pH 6.8. Ascending phosphate concentration

steps (0.1 M and 0.2 M sodium phosphate buffer at pH 6.8) were used as elutions. The majority of OPN (61%) was eluted with 0.1 M sodium phosphate buffer also at pH 6.8. The rest of OPN was all recovered in the second step using 0.2 M sodium phosphate. Similarly, all the protein adsorbed was eluted in two steps by 0.1 M and 0.2 M sodium phosphate respectively (Figure 6). Despite the exhibited adsorption selectivity for OPN, CHT failed to show greater purification capacity than HIC (Phenyl Sepharose) resin. The achieved purification fold of OPN with CHT was only 2.3 fold.

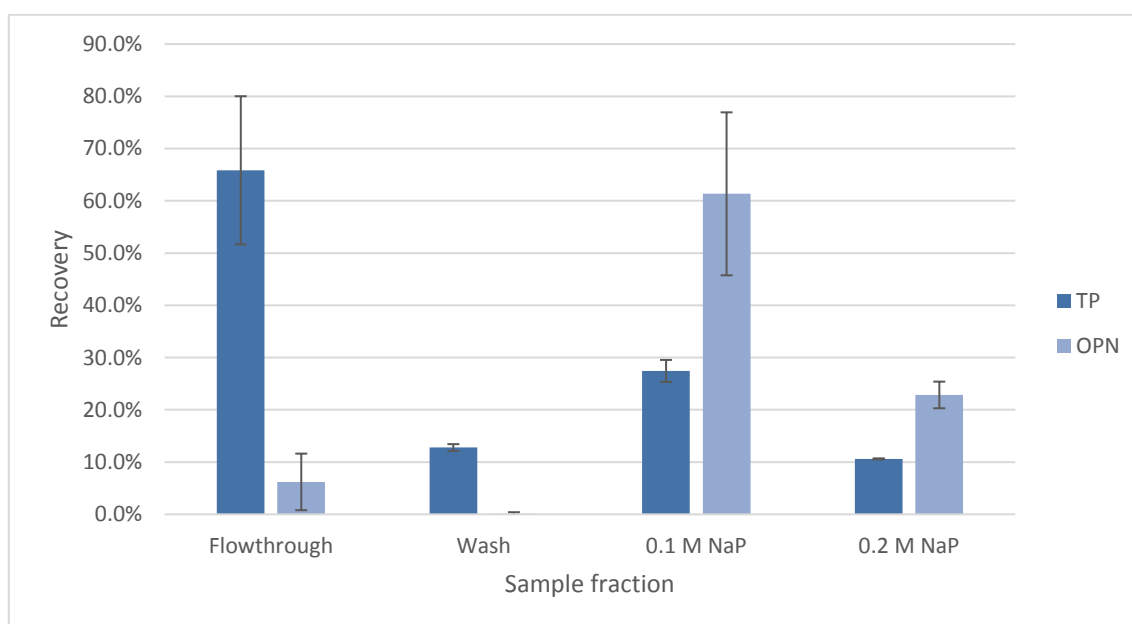


**Figure 6** Batch adsorption and elution of OPN and total proteins (TP) using ceramic hydroxyapatite. Adsorption was performed from *E. coli* clarified lysate dialyzed against 5 mM sodium phosphate buffer at pH 6.8. Elution 1: 0.1 M sodium phosphate buffer pH 6.8; Elution 2: 0.2 M sodium phosphate buffer pH 6.8.

### 3.1.4 OPN adsorption and elution studies with mixed-modal resins

The acidic and hydrophobic nature of OPN led us to search for an efficient capture resin among the mixed-modal resins that possess anionic and hydrophobic interaction properties. Commercial mixed-modal chromatography sorbents that were evaluated include Cpto adhere (GE Health), HEA Hypercel, PPA Hypercel and MEP Hypercel (Pall). Resin performance was judged based on OPN recovery yield and purification factor.

#### 3.1.4.1 HEA HyperCel adsorption/elution study

HEA HyperCel has cellulose based matrix with hexylamine ligand. This ligand has strong anionic ( $pK_a \sim 10$ ) and hydrophobic properties at neutral pH, which allows protein capture under physiological conditions<sup>38</sup>.

To investigate the interaction between OPN and the HEA ligand, high-throughput screening (HTS) experiments were conducted in the pH range from 5 to 9 and salt concentrations from 0 to 3 M NaCl. The unbound OPN and total TP after equilibrium adsorption were quantified by ELISA and Bradford assay<sup>53</sup> respectively. Response surface analysis was carried out by JMP Software and the prediction profiles of OPN and TP bound to HEA resin are shown as Figure 7.

The contour profile of OPN adsorption (Figure 7A) shows that OPN adsorption increased in the whole pH range (pH 5 to 9) at any given salt concentration within the tested range. Salt concentration had a significant and interesting effect on OPN adsorption to HEA HyperCel sorbents. At salt concentrations below 0.5 M, the majority of OPN bound to the HEA primarily by electrostatic interaction. As the salt (NaCl)

concentration increased to 1 M range, charge interaction was substantially weakened resulting in reduced OPN bound fraction by as much as 50%. In the high-salt range (NaCl concentration >2.5 M) where hydrophobic interaction became more prevalent, adsorbed OPN fraction back to 70% - 90% level. The impact of pH and NaCl concentration on total protein is less dramatic than on OPN (Figure 7B), which is expected since the proteome of *E. coli* consists host cell proteins (HCPs) with different properties that would lead to different responses to HEA ligand according to different conditions. Generally, higher NaCl concentration led to higher amount of adsorption.

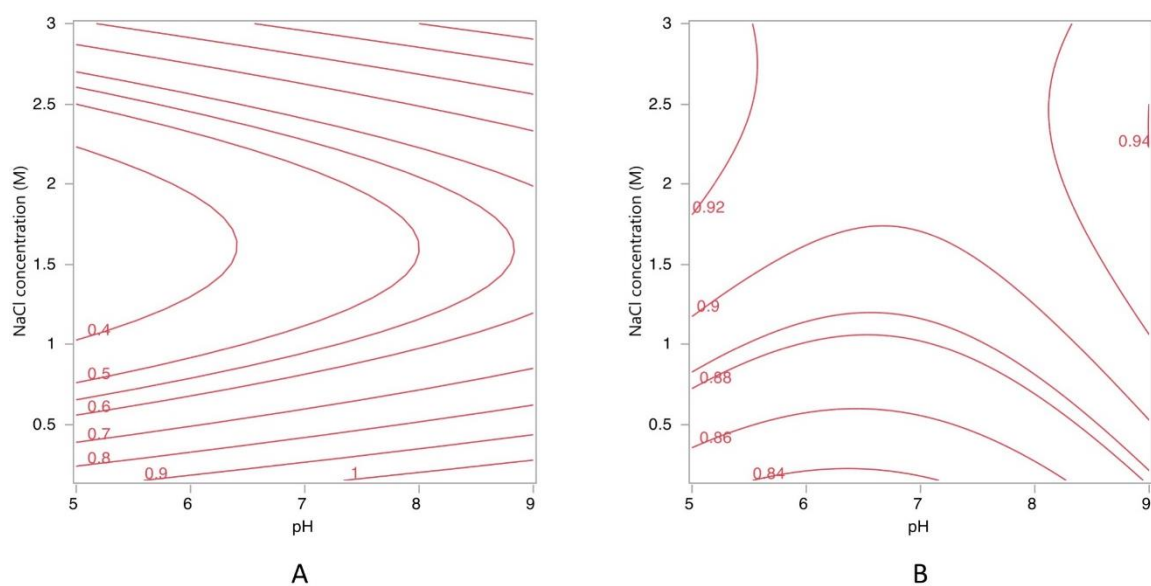


**Figure 7** Contour profile of OPN (A) and total protein (B) bound to HEA HyperCel. Numbers on the contour grids represent the fraction of protein in the lysate that was adsorbed to HEA Hypercel.

The HTS results suggest that both high salt (3 M NaCl) and low salt condition (close to 0.1 M NaCl) would favor OPN adsorption in the whole pH range (5 to 9). Two (high and low-salt) adsorption conditions were selected for further investigation. For the batch adsorption under low salt condition, the clarified cell lysate was incubated directly with HEA resin for 1 hour at room temperature as described in Materials and Methods section. No resin conditioning was required as HTS results in Figure 7A predicted more than 90% of OPN would be bound from pH 7 50 mM Tris buffer containing 150 mM NaCl.

Based on the screening results, we designed a 3-step elution process for complete desorption of OPN using a combination of pH and salt concentration changes that gradually weakened hydrophobic and charge interactions and eventually led to electrostatic repulsion. The elution steps consisted of 50 mM Tris buffer at pH 7 containing 1 M NaCl, followed by pH 5 0.1 M sodium acetate buffer with 1 M NaCl and pH 3 0.1 M sodium citrate buffer without NaCl addition. The recovery of OPN and total soluble protein from the initial loading sample in each step are shown in Figure 8.

As predicted by HTS data at pH 7, very small amount of OPN (5%) was detected in the flowthrough fraction, whereas more than 40% of *E. coli* total protein did not bind to HEA and remained in the flowthrough. After resin washing with the binding buffer, NaCl concentration was increased to 1 M for the first elution step while keeping the pH at 7. Because the majority of bound OPN (76%) was desorbed under those conditions and only 6% of the bound *E. coli* protein, this step alone resulted in 14-fold purification of OPN. While the rest of adsorbed OPN was recovered in the subsequent elution steps,

only 45% of *E. coli* proteins initially bound to HEA HyperCel were recovered. Complete desorption of strongly adsorbed proteins and regeneration of HEA would probably require using of 1 M NaOH.

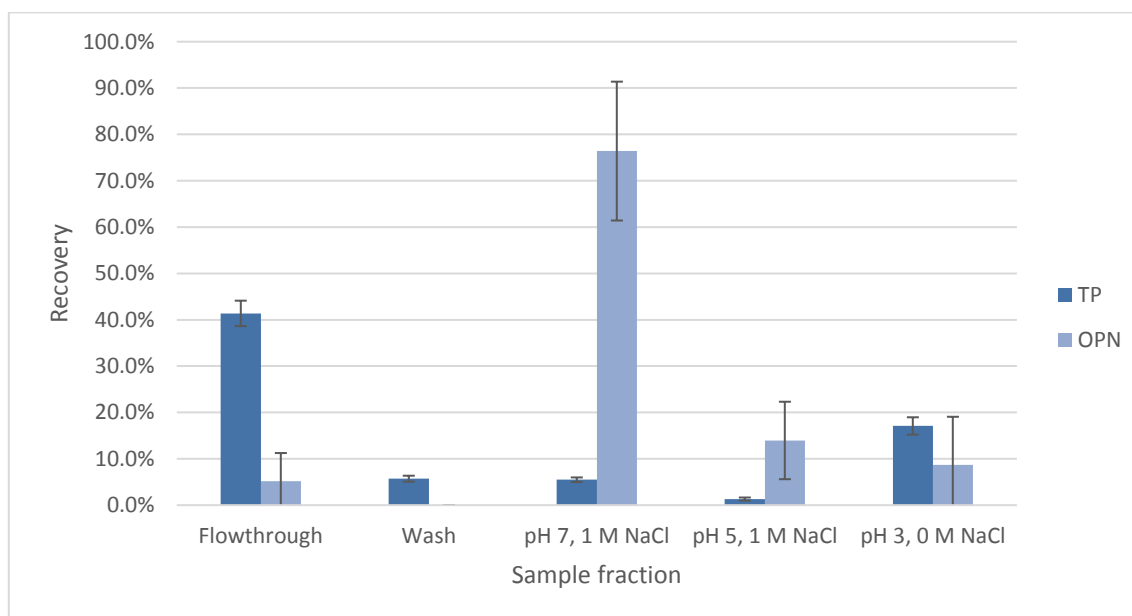


**Figure 8** Low-salt batch adsorption and elution of OPN and *E. coli* total proteins using HEA HyperCel: Adsorption was performed from pH 7 *E. coli* clarified lysate containing 150 mM. Elution steps are pH 7 with 1 M NaCl, pH 5 with 1 M NaCl, and pH 3 with no NaCl addition.

For adsorption experiments at high-salt, the resin was conditioned with the binding buffer (3.0 M NaCl, 50 mM Tris, pH 7) and clarified lysate (pH 7) was adjusted to 3.0 M NaCl concentration before incubation. The same elution steps and conditions as in the low salt adsorption experiments were applied (Figure 9).

Under high salt conditions, hydrophobic interactions were the dominating factor. Compared to low-salt binding, more than 80% of *E. coli* protein was bound to HEA resin (less than 20% detected in the flowthrough) and 92% OPN was bound. After resin wash



with 10 column volumes of binding buffer, the first elution was done with 1 M NaCl at pH 7. The majority of OPN (74%) and 10% of *E. coli* protein were desorbed in the first elution step achieving 7-fold purification of OPN in a single step. The rest of the bound OPN was recovered in the two subsequent elution steps (Figure 9) but the residual 58% of *E. coli* proteins remained tightly bound to the resin.

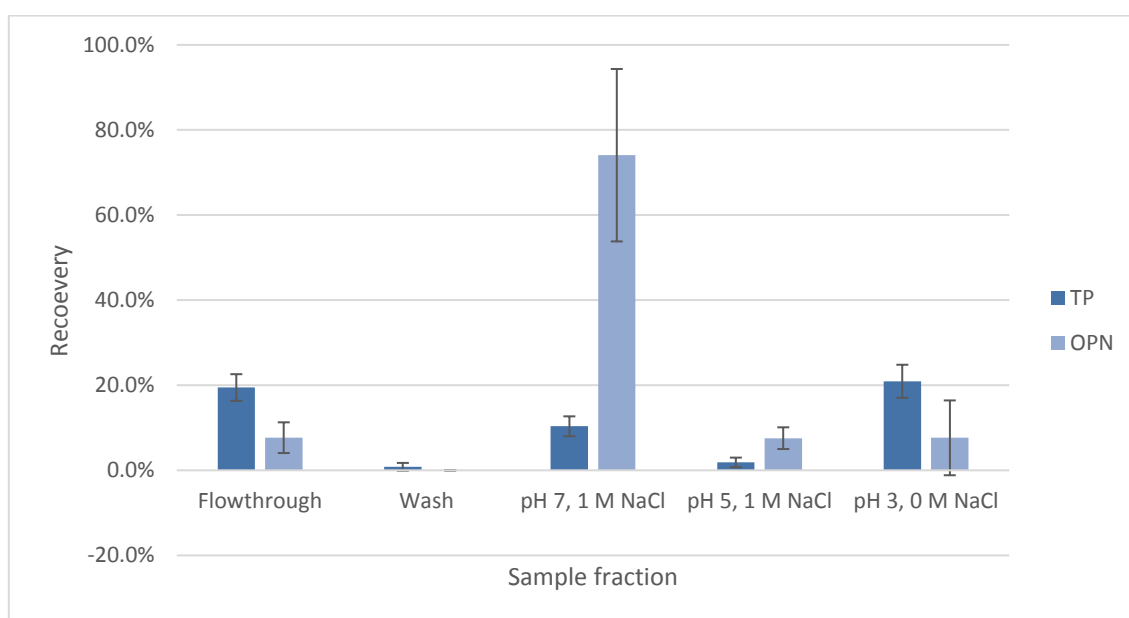


**Figure 9** High-salt batch adsorption and elution of OPN and *E. coli* total soluble protein using HEA HyperCel: Adsorption was performed from conditioned *E. coli* clarified lysate with 3 M NaCl pH7. Elution steps were pH 7 with 1 M NaCl, pH 5 with 1 M NaCl, and pH 3 with no NaCl addition.

### 3.1.4.2 PPA HyperCel adsorption studies

PPA HyperCel is another mixed-modal adsorbent with phenylpropylamine ligand (Table 4). The same set of HTS experiments was performed with PPA as previously with

the HEA HyperCel resin. The prediction contour profile of OPN bound to the PPA HyperCel is shown in Figure 10.

Total protein behaved similarly on PPA HyperCel compared to HEA HyperCel reflecting the similarity of the ligand structure. However, over 90% of OPN was retained by PPA HyperCel under all the tested conditions. Clearly, the aromatic ring from PPA ligand provided much higher affinity for OPN than the aliphatic group from HEA.

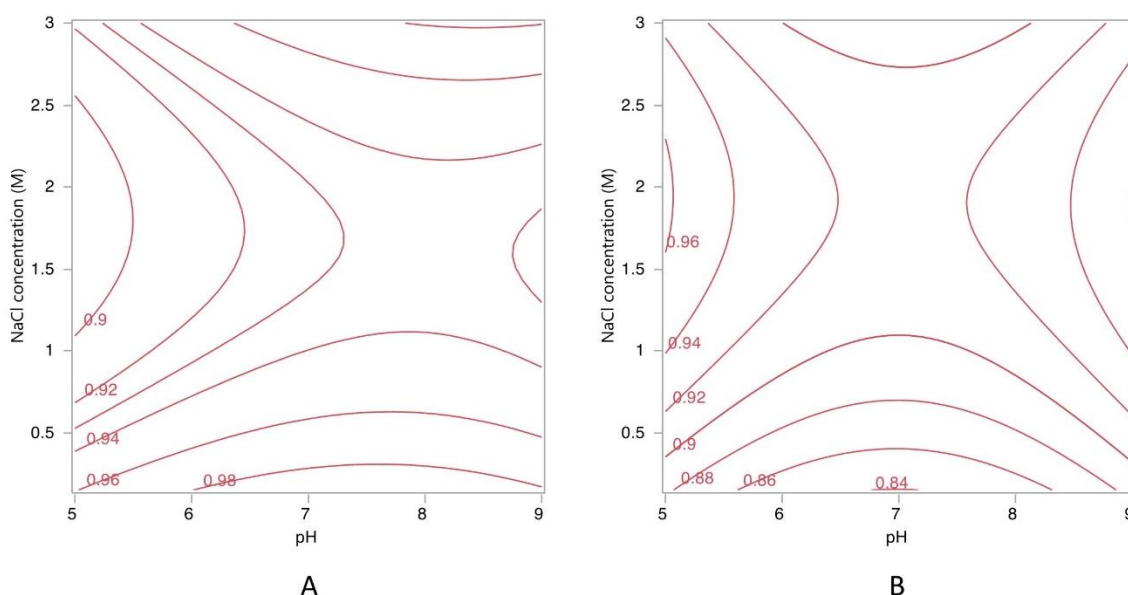


**Figure 10** Contour profile of the proportion of OPN (A) and total protein (B) bound to PPA HyperCel. Numbers on the contour grids represent the fraction of protein in the lysate that was adsorbed to PPA HyperCel.

The elution of adsorbed protein from PPA HyperCel was tested using exactly the same pH and salt conditions as with HEA HyperCel. As predicted by HTS, the *E. coli* proteins behaved similarly on both PPA HyperCel and HEA HyperCel resins but the OPN distribution in the eluted fractions was different. A small fraction of OPN was recovered in the first elution step (pH 7, 1 M NaCl) and almost none in the second. The majority of OPN (60%) was desorbed from PPA HyperCel at pH 3. Unfortunately, the

pH 3 elution fraction also contained a significant amount of *E. coli* host cell proteins, which led to lower purification factors (3-fold purification for low-salt binding conditions and 2.5-fold for high salt binding). No significant difference in the adsorption and elution profiles of OPN and total protein was observed between low salt (Figure 11) and high salt binding concentrations (Figure 12).

Although 90% of OPN could be eluted from PPA HyperCel resin during pH 7 and pH 3 elution, more than 60% of total protein remain adsorbed.

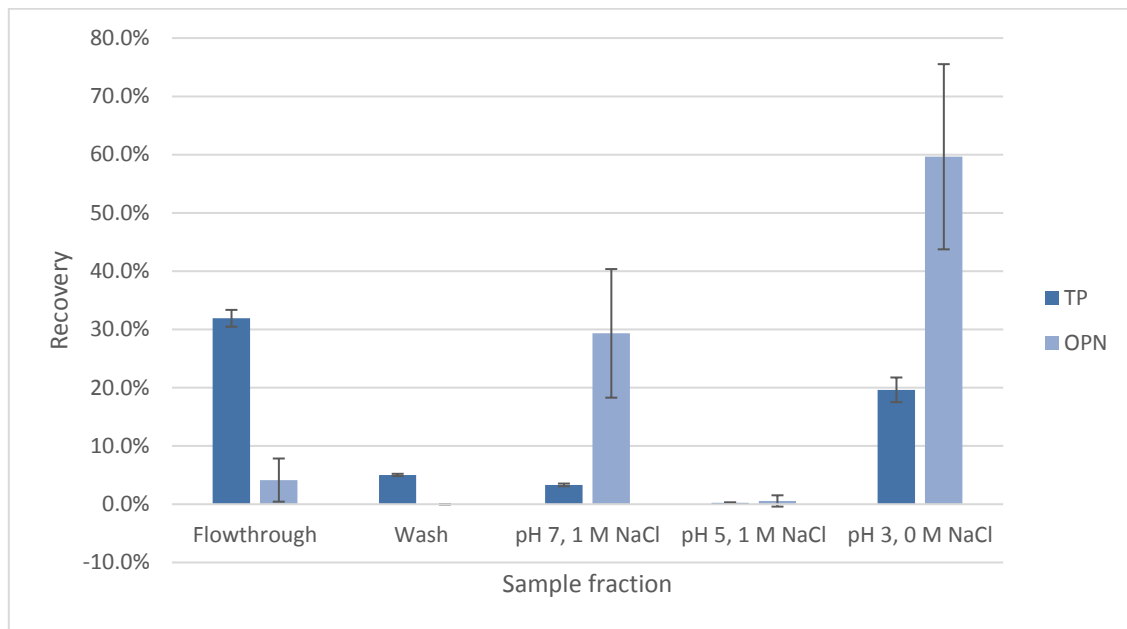


**Figure 11** Low-salt batch adsorption and elution of OPN and *E. coli* total soluble protein using PPA HyperCel: Adsorption was performed from *E. coli* clarified lysate containing 150 mM NaCl pH 7. Elution steps were pH 7 with 1 M NaCl, pH 5 with 1 M NaCl, and pH 3 with no NaCl addition.

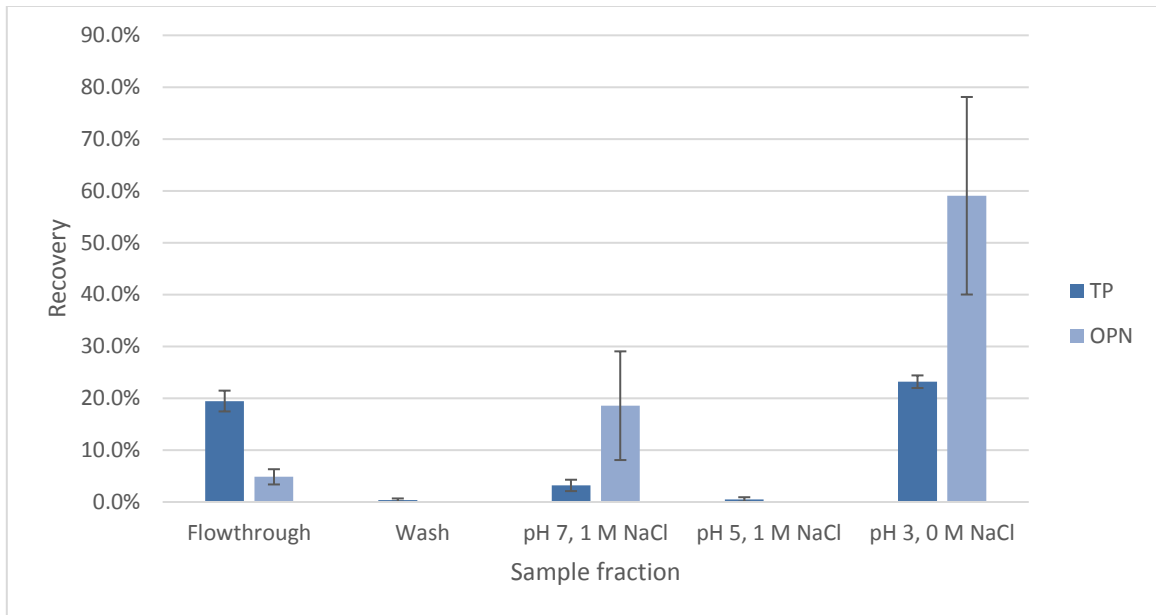


**Figure 12** High-salt batch adsorption and elution of OPN and *E. coli* total protein using PPA HyperCel: Adsorption was performed from conditioned *E. coli* clarified lysate containing 3 M NaCl at pH 7. Elution steps are pH 7 with 1 M NaCl, pH 5 with 1 M NaCl, and pH 3 with no NaCl addition.

### 3.1.4.3 Capto adhere adsorption studies

Capto adhere is a strong multimodal anion exchanger (N-benzyl-n-methyl ethanolamine) designed to bind proteins via ionic, hydrogen, and hydrophobic interactions. The hydrophobicity of Capto adhere ligand is reported to be reduced by the presence of multiple hydroxyl groups<sup>38</sup>. HTS designed similarly to HEA and PPA resin screening were carried out to investigate interaction between OPN and Capto adhere. As shown in Figure 13, NaCl a concentration had significant impact on OPN adsorption to Capto adhere. The fraction of adsorbed OPN decreased with the increase of NaCl concentration indicating that the predominant interactions between OPN and Capto adhere ligands were ionic. OPN binding with Capto adhere at high pH condition was also tested. Unlike HEA Hypercel, the hydrophobic interaction failed to take over even

when NaCl concentration increased to 3 M. At pH 7 and 3 M NaCl, more than 70% of OPN remained in the flowthrough fraction (data not shown). Therefore, salt removal by dialysis/diafiltration was a necessary conditioning step for OPN adsorption to Cpto adhere from *E. coli* lysate.

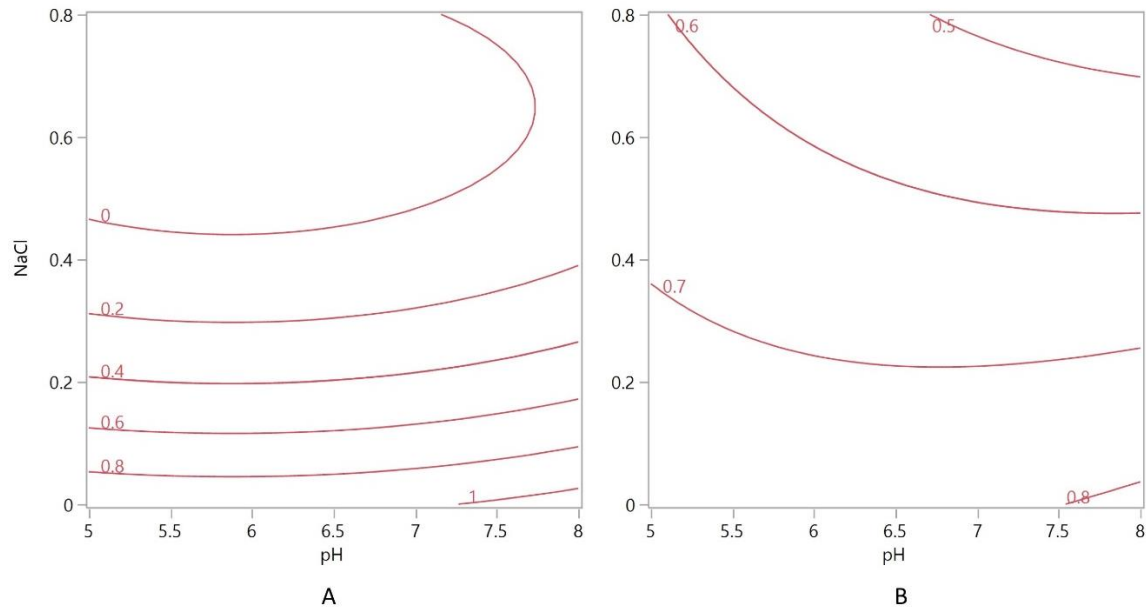


**Figure 13** Contour profile of the proportion of OPN (A) and total protein (B) bound to Cpto adhere. Numbers on the contour grids represent the fraction of protein in the lysate bound to the Cpto adhere.

Adsorption and elution experiments were carried out using dialyzed cell lysates. Preliminary elution data established that stepwise protein desorption with a descending pH buffer (0.1 M citrate- phosphate buffer at pH 5, 4 and 3), suggested by the resin vendor (GE Healthcare), was optimal for purification of OPN. Around 8% of OPN and 30% of host cell protein remained in the flowthrough (Figure 14). After the resin wash step with the binding buffer, additional 16% of host cell proteins were eluted at pH 5 and pH 4 and less than 2% of OPN at pH 4. The majority of OPN (78%) was recovered in

the third elution step when the buffer pH was lowered to 3, a pH below OPN pI. During this last stage about 17% of *E. coli* total protein co-eluted with OPN, which resulted in 4.6-fold OPN purification. Contrary to traditional strong anion exchanger such as Capto Q, only 51% of *E. coli* protein adsorbed to Capto adhere could be recovered, which indicates the benzene ring provides additional binding capacity to the quaternary amine. And recycling the sorbent would require deep cleaning.

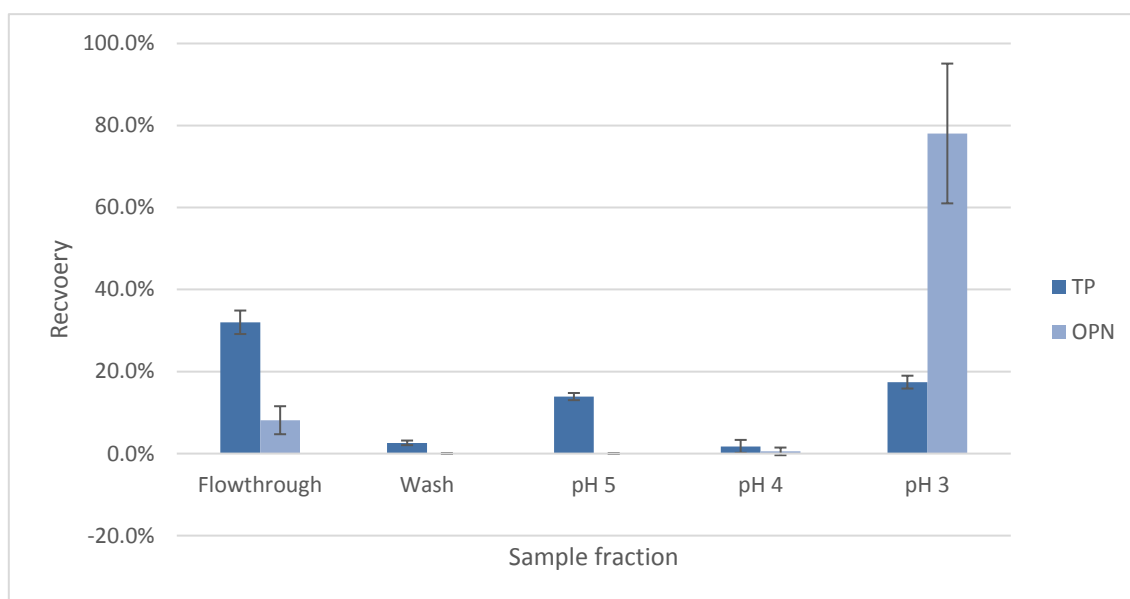


**Figure 14** Batch adsorption and elution of OPN and *E. coli* total soluble protein by Capto adhere, *E. coli* clarified lysate was dialyzed to remove salt before adsorption. Binding condition: pH 7 50 mM Tris Buffer. Elution 1 - 3: Citrate-phosphate buffer pH 5, pH 4, pH 3.

#### 3.1.4.4 MEP HyperCel adsorption studies

MEP HyperCel is another sorbent from the HyperCel cellulosic matrix family. The ligand has a relatively low pKa of 4.8 and does exhibit a significant anionic properties below pH 5. Based on our preliminary adsorption studies, MEP ligand (4-

mercapto-ethyl- pyridine) appears to be more hydrophobic than traditional HIC resin such as Phenyl Sepharose. Thus, 0.5 M ammonium sulfate or 3.0 M sodium chloride was sufficient to promote OPN adsorption. These salt concentrations resulted in substantially less OPN precipitation than 1.0 M ammonium sulfate required for OPN adsorption to Phenyl Sepharose.

We tried several elution strategies by various combinations of pH and salt concentrations and determined that OPN could not be recovered in a single fraction. The OPN recovery by decreasing pH and salt concentration is presented in Figure 15. The fraction with the highest OPN yield of 40% was recovered during the second elution step (pH 5 containing 1 M NaCl). This pool, contained 14% of *E. coli* total proteins, achieved three-fold purified OPN. Similar to the other two HyperCel resins, only half (53%) of the total protein bound to MEP and almost 100 % OPN were recovered in the three elution steps (Figure 15). Intensive cleaning and regeneration protocols are needed here for resin recycling.

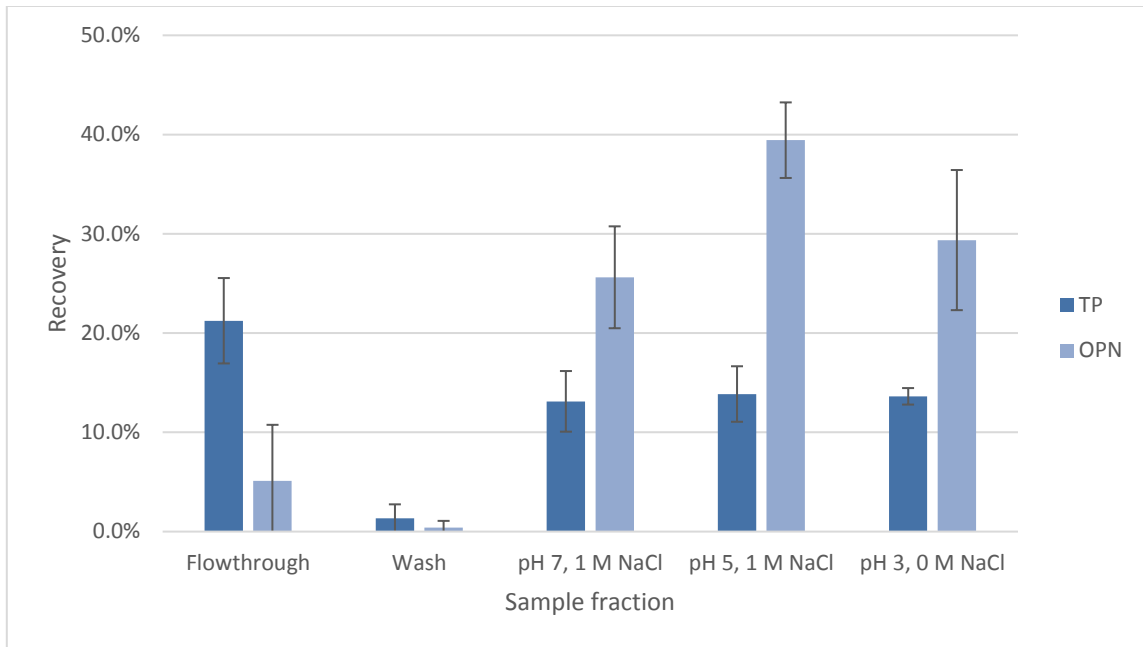


**Figure 15** Batch adsorption and elution of OPN and *E. coli* total protein using MEP HyperCel: Adsorption was performed from pH 7 *E. coli* clarified lysate containing 3 M NaCl. Elution steps are pH 7 with 1 M NaCl, pH 5 with 1 M NaCl, and pH 3 without NaCl addition.



### 3.1.5 Resin performance evaluation and comparison

All the batch adsorption and step elution experiments were done in triplicates with similar loading capacities. OPN recovery and purification fold data in Table 6 were normalized against the initial protein content in the conditioned cell lysate (feed).

Least square fitting test was carried out to test the effects of resins on OPN recovery and purification factors. As a result, the effect of the type of resins on OPN recovery has a P-value of 0.0168, which means different resins yielded significantly different OPN recovery. The P-value of OPN purification factor given by JMP Pro was less than 0.0001 suggesting the different resins performed dramatically different in terms of OPN purification. The variation due to the date of experiment contributed 38% and 50% of variance to OPN recovery and purification factor respectively, according to REML (residual maximum likelihood) variance component estimates given by JMP Pro, which means day-to-day variation had significant effects on response and blocking it was necessary to help isolating the effects of type of resins on OPN recovery and purification. This day-to-day variation was most likely due to that the sonication for protein extraction was not ideally robust. High pressure homogenization would be a more robust protein extraction method that could help solve this issue introduced by sonication when the process was scaled-up to the point where homogenization were applicable.

Knowing that different resins significantly yielded different OPN recovery and purification factors, each pair Student's test at 95% confidence ( $\alpha = 0.05$ ) were carried out on the least square means of OPN recovery and purification factor to compare the

performance between resins. The results were given in connecting letters reports. The letters were marked in Table 6. The resins having the same letter marked on the recovery or purification factor had no significantly different performance in terms of OPN recovery or purification respectively.

The binding and eluting conditions, purification factors, and OPN recoveries are presented in Table 6 for comparison. The data in Table 6 includes a single OPN elution step that yielded the highest recovery although in several cases achieving the highest OPN purification fold required additional elution steps.

The ranking of resins in Table 6 was primarily based on purification factor for the OPN specific recovery and OPN recovery was also taken into account during the ranking process. The top resin candidates for further process development and scale up are HEA HypeCel (low salt lysate), Capto Q, and HEA HyperCel (high salt lysate). HEA HyperCel (low salt lysate) ranked first thanks to its exceptional 14-fold purification and its 76% recovery was among the highest as well. HEA HyperCel efficiently captured OPN directly from the clarified cell lysate without any additional lysate conditioning steps. From a manufacturing view point, direct OPN capture would save operating time and expenses associated with conditioning of a large volume-low initial purity OPN extracts.

Capto Q was ranked at the second place because its 92% recovery is the highest in all candidates. And the 6-fold purification achieved by Capto Q was just shy from the 14-fold from HEA HyperCel but significantly higher than other resins tested. It should be noted that achieving a 6-fold purification with Capto Q required resin wash with 50

mM Tris buffer, pH 7 containing 0.2 M NaCl to remove 44% of co-adsorbed *E. coli* proteins (Figure 4). The least amount of OPN that remained unbound after equilibrium adsorption is an indication of resin's high binding capacity. The requirement for a salt removal step and an intermediate wash step was the major downside of Capto Q when compared with HEA HyperCel.

HEA HyperCel (high salt) was the third best performer due to its 7-fold purification and a decent 74% recovery. The fact that HEA HyperCel worked under two vastly different conditions reveals the potential and versatility of the resin.

The rest of the candidates resulted in significantly lower purification factors, so they were not chosen for further development.

**Table 6** Comparison of resins by batch purification experiments, their respective purification factors and recoveries. Recovery and purification factors are expressed as mean  $\pm$  standard deviation. Values having the same letters are not significantly different.

<b>Resin</b>	<b>Binding Condition</b>	<b>OPN Elution Condition</b>	<b>Purification Factor</b>	<b>Recovery (%)</b>
<b>HEA HyperCel (Low-Salt)</b>	50 mM Tris, pH 7, 0.15 M NaCl	50 mM Tris, pH 7, 1 M NaCl	13.99 $\pm$ 2.86 <sup>A</sup>	76.4 $\pm$ 15.0 <sup>A,B</sup>
<b>Capto Q</b>	50 mM Tris pH 7	50 mM Tris pH 7, 0.5 M NaCl	5.92 $\pm$ 0.73 <sup>B,C</sup>	92.0 $\pm$ 15.4 <sup>A</sup>
<b>HEA HyperCel (High-Salt)</b>	50 mM Tris, pH 7, 3 M NaCl	50 mM Tris, pH7, 1 M NaCl	7.10 $\pm$ 2.98 <sup>B</sup>	74.1 $\pm$ 20.3 <sup>A,B</sup>
<b>Capto adhere</b>	50 mM Tris pH 7	pH 3 citrate phosphate buffer	4.61 $\pm$ 0.73 <sup>C,D</sup>	78.1 $\pm$ 17.0 <sup>A,B</sup>
<b>PPA HyperCel (Low-Salt)</b>	50 mM Tris, pH 7, 0.15 M NaCl	0.1 M sodium citrate, pH 3	3.05 $\pm$ 0.87 <sup>C,D,E</sup>	59.6 $\pm$ 15.9 <sup>B,C</sup>
<b>Phenyl Sepharose</b>	50 mM Tris, pH 7, 1 M ammonium sulfate	50 mM Tris, pH 7, 0.5 M ammonium sulfate	2.88 $\pm$ 0.69 <sup>D,E</sup>	71.2 $\pm$ 21.9 <sup>A,B</sup>
<b>PPA HyperCel (High-Salt)</b>	50 mM Tris, pH 7, 3 M NaCl	0.1 M sodium citrate, pH 3	2.48 $\pm$ 1.19 <sup>E</sup>	59.1% $\pm$ 19.0% <sup>B,C</sup>
<b>CHT</b>	5 mM Phosphate, pH 6.8	0.1 M Phosphate, pH 6.8	2.34 $\pm$ 0.36 <sup>E</sup>	61.3% $\pm$ 15.6% <sup>B,C</sup>
<b>MEP HyperCel</b>	50 mM Tris, pH 7, 3 M NaCl	0.1 M Sodium acetate pH 5, 1 M NaCl	2.82 $\pm$ 1.01 <sup>D,E</sup>	39.4% $\pm$ 3.8% <sup>C</sup>

### 3.1.6 Resin performance verification and optimization on packed-bed columns

To confirm the validity of batch adsorption results, the processes used in batch adsorption experiments were repeated using packed-bed columns operated by ÄKTA Purifier chromatography system. The best resin candidates from Table 6 (HEA and Capto Q) were tested in a packed-bed adsorption configuration. The same feed composition and load volume was used on 1-ml prepacked columns (PRC HEA HyperCel 1 ml, HiTrap Capto Q 1 ml) to allow the comparison of achieved purification fold and OPN recovery between batch adsorption and packed-bed chromatography. The flow rate was controlled at 0.2 ml/min to ensure a 5-minute residence time during binding, and kept constant throughout wash and elution processes.

For HEA HyperCel under low salt binding conditions, 6 ml of clarified lysate was directly loaded to equilibrated PRC HEA HyperCel column (1 ml). After 20 column volumes of wash with loading buffer, linear NaCl concentration gradient elution (0.15 M – 1.5 M NaCl over 20 column volumes, in pH 7 50 mM Tris buffer) was carried out. The OPN concentrations in the collected fractions determined by ELISA were plotted in Figure 16. OPN concentration followed the same trend as the A280 peak which reached maximum at buffer containing 1 M NaCl. The pooled (36-50 ml, 0.6 M NaCl to 1.1 M NaCl) fractions contained 97% of loaded OPN amount compared to 76.4 % from the batch adsorption. The difference between column gradient and step desorption in terms of OPN yield was that the reported 76.4% referred to OPN yield obtained from the single 1 M NaCl step (Figure 8). Two additional elution steps, after the 1 M-NaCl step, increased the OPN recovery from 76.4 % to 93%. Gradient elution from packed-bed

HEA column resulted in 16-fold purification – a value similar to 14-fold achieved by 1 M NaCl step. In summary, the gradient elution of OPN from HEA was apparently more efficient probably because of the higher salt concentration reaching 1.2 M NaCl in fraction 52 mL.

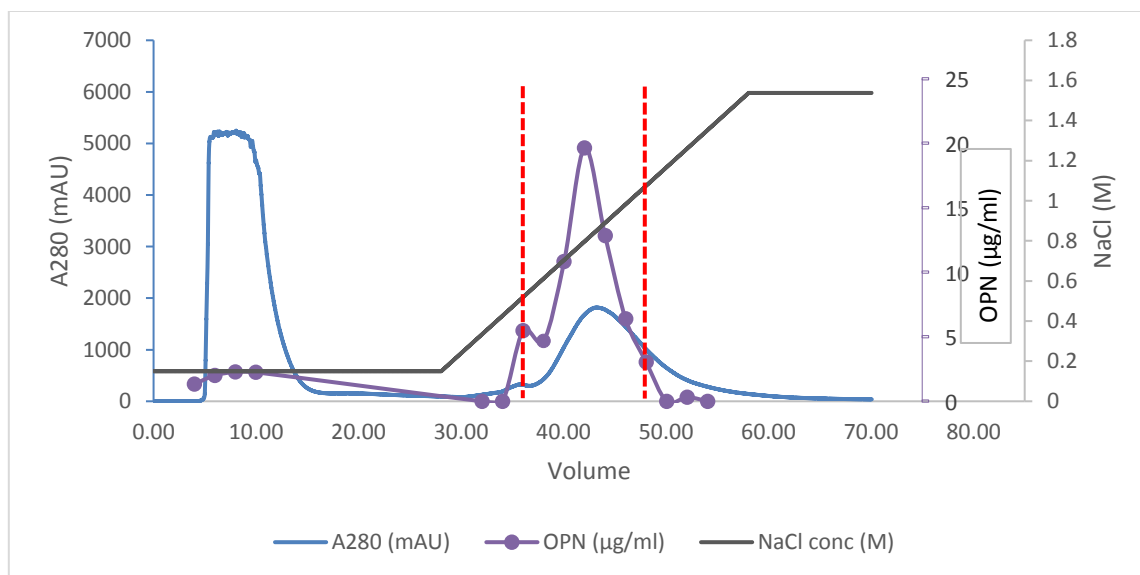


**Figure 16** Chromatogram of HEA HyperCel low salt bind/elute operated by ÄKTA system. OPN eluted in the peak around 1 M NaCl illustrated between the red-dotted lines.

HEA HyperCel packed bed column experiments using high-salt containing lysate did not work because of back-pressure build-up during loading. We believe the pressure build up was caused by the protein aggregation on the column, and decided not to proceed with the development of OPN purification under high-salt (3 M NaCl) binding conditions.

Packed-bed purification of OPN with Capto Q resin was carried out after the dialysis of clarified lysate. The lysate ionic strength was reduced to below 5 mS/cm, as

determined in batch experiments, for maximal adsorption of OPN. The OPN elution was performed with a linear salt gradient (0 M to 1 M NaCl) over 20 column volumes. The majority of OPN was recovered in the 2 fractions (44 to 46 mL) at conductivities between 32 mS/cm and 49 mS/cm which correspond to 0.26 M and 0.45 M NaCl concentrations in 50 mM Tris buffer. The pooled protein fractions (43-46 mL) contained 90% of the loaded OPN. The purity of OPN in this pool reached 22% resulting in 11-fold purification, which is significantly higher than 6-fold achieved by step elution with 0.5 M NaCl (Figure 4).

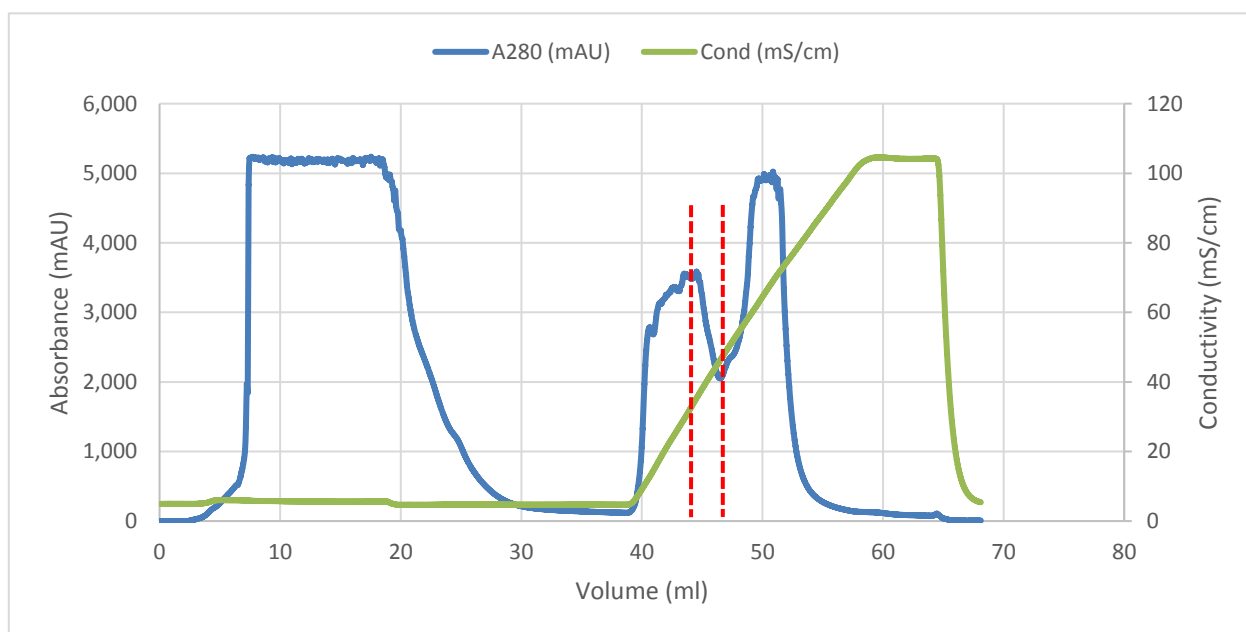


**Figure 17** Chromatogram of anion exchange chromatography. Dialyzed *E. coli* lysate loaded on HiScreen Capto Q column. Elution by ascending NaCl concentration linear gradient. OPN eluted between 0.26 M and 0.45 M NaCl illustrated between the red-dotted lines.

Compared with batch adsorption results, prepacked columns on ÄKTA resulted in higher yield and purification fold. In batch adsorption experiments, the resins were not tightly packed resulting in back mixing. In addition to the lack of control over flow rate, there were significantly more variations in elution conditions and fraction collection for batch adsorption experiments than packed-bed chromatography on ÄKTA system. For Capto Q purification, the shortage of control over elution conditions and flowrate in batch adsorption experiments kept the process development from approaching small margin of condition optimization (0.2 M NaCl and 0.5 M NaCl elution steps in Figure 4) and ended up with lower purification factor (6 fold) than precisely controlled linear gradient and fraction collection by ÄKTA (OPN eluted between 0.26 M and 0.49 M NaCl with 11 fold purification). For HEA HyperCel the difference in adsorption mode (equilibrium binding vs dynamic binding) also contributed to the variability.

Despite the variabilities, the results of batch adsorption experiments and prepacked columns on ÄKTA were comparable, indicating that batch adsorption and elution experiments in conjunction with HTS of resins could be used as a fast and low-cost process development tool.

It appears that HEA HyperCel (low salt) has better specificity for capturing OPN from crude and salt-containing *E. coli* lysates than Capto Q. On the other hand, Capt Q has high-adsorption capacity that would allow a significant OPN concentration from low-expressing *E. coli* strains.



### **3.2 Two-step OPN purification process design**

Since both resins demonstrated capture and purification potential, we tested their application in two orthogonal OPN purification trains: HEA followed by CaptoQ and CaptoQ followed by HEA processes.

#### *3.2.1 OPN purification by HEA-Q process*

In this purification scheme, HEA HyperCel served as the OPN capture step and Capto Q as a purification step. The clarified lysate was directly loaded to PRC HEA HyperCel (1 ml) column at linear velocity of 60 cm/h and washed by 20 column volumes of loading buffer. Since no separation of OPN from host protein was achieved by gradient elution i.e. a single peak containing HCPs and OPN in (Figure 16), one step elution with 50 mM Tris buffer, pH 7, containing 1 M NaCl was applied. The main driver for choosing a step elution over gradient was to obtain a higher-protein concentration pool and reduce elution buffer volume from 14 ml to 8 ml, the latter being important only on a manufacturing scale (Figure 18).

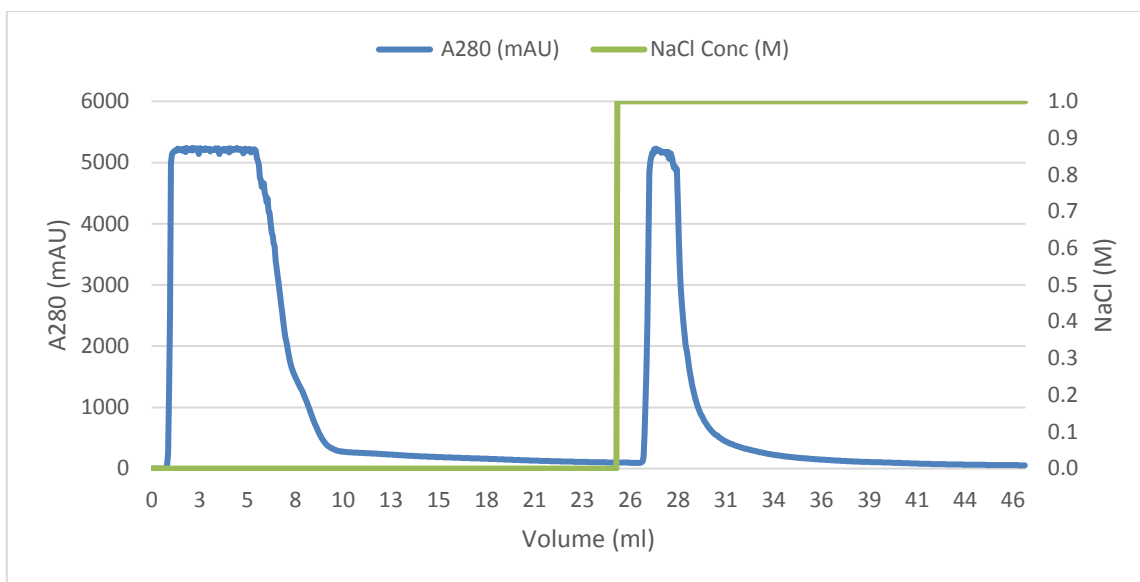


**Figure 18** Chromatogram of HEA HyperCel low-salt binding and step elution. The elution peak was collected for Capto Q purification (23-31 ml).

The partially purified OPN from HEA HyperCel elute was loaded to HiTrap Capto Q column (1 ml) after salt removal by dialysis. Dialyzed HEA eluate (conductivity <5 mS), was loaded on HiTrap Capto Q (1ml) as before, washed with 20 column volumes of the binding buffer (50 mM Tris, pH 7, 4 mS). After the wash procedure, 0 – 1 M NaCl linear gradient elution (20 CV) was applied to Capto Q as for further separation of OPN from *E. coli* HCPs. The linear NaCl concentration gradient generated 3 major peaks as depicted Figure 19. OPN was recovered in the second peak and marked between the red dotted lines in Figure 19 with improved purity. The details of OPN purification achieved by this process are given in Figure 20 and the purification table (Table 7).

The capture step by HEA HyperCel yielded 81% recovery and elevated OPN purity from 2% in the crude lysate to 29%. The dialysis step was the necessary condition

step between chromatography steps and unfortunately caused 40% loss in a single step. The second purification step by Capto Q prove to be an orthogonal step to HEA and continue to purify OPN from 29% to 95% with 90% recovery. Overall, this 2-step purification process yielded 44% recovery with over 95% purity when considering the OPN fragment (Figure 20) which requires additional steps to remove if needed by specific application.

This process took advantage of the salt-tolerant adsorption property of HEA HyperCel to eliminate conditioning step on the large-volume and low-purity lysate before capture chromatography. However, the HEA HyperCel pool contained 1 M NaCl that required extensive dialysis to remove. A significant OPN loss was observed during dialysis presumably due to protein binding to the dialysis membrane. The decrease of purity from 29% to 20% indicates that OPN was lost and less of *E. coli* HCPs. Because to OPN was not detected by ELISA in the dialysis buffer, we concluded that it was due to binding to the membrane. Several attempts to increase the yield seem to indicate that low sample volume to dialysis surface area ratio might be the cause for low recovery. On a larger scale, salt removal could be achieved by diafiltration on a tangential flow systems which should reduce protein loss for its much smaller surface area to volume ratio and the presence of constant sheer force.

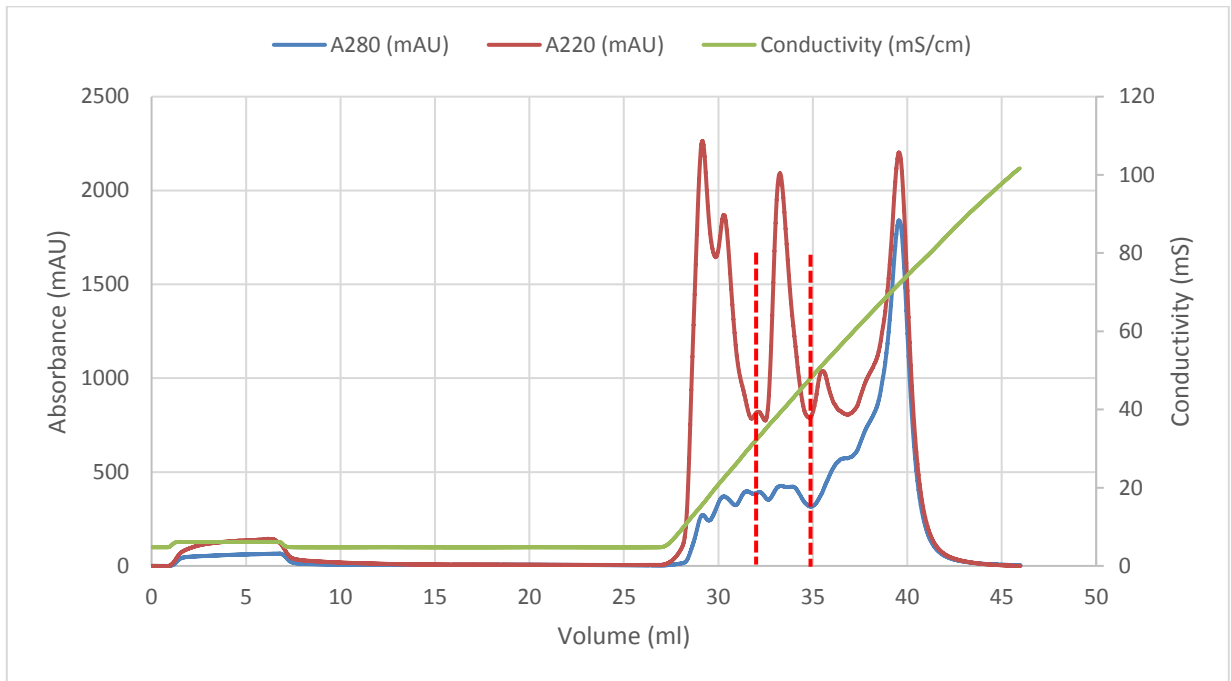


**Figure 19** Chromatogram of OPN purification on Capto Q following HEA HyperCel capture.

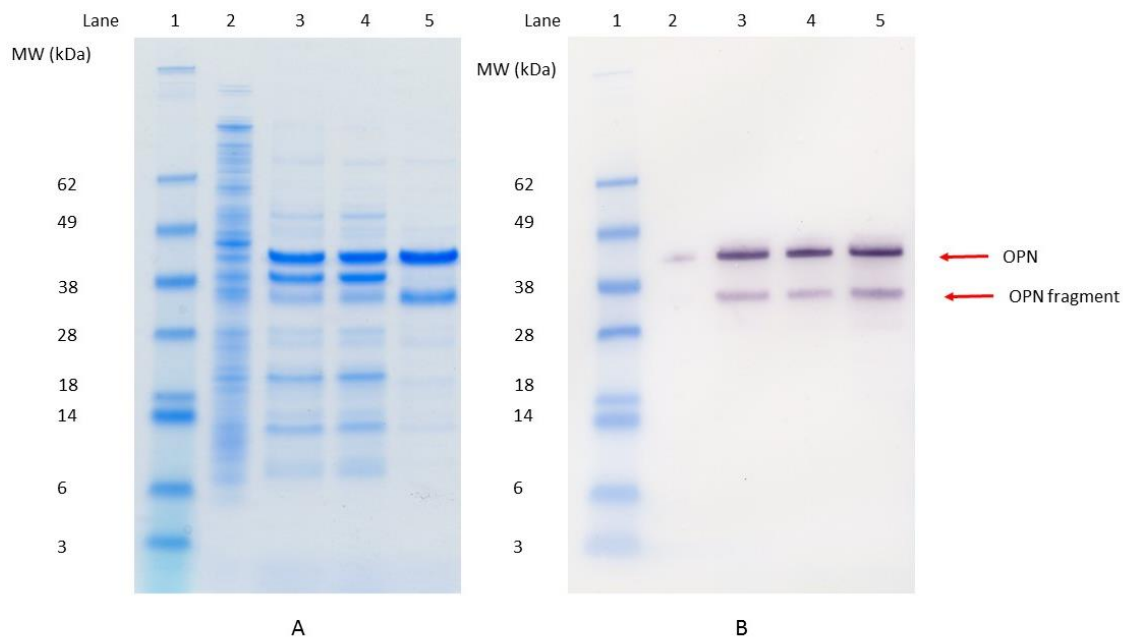


**Figure 20** Purification of OPN by HEA and Capto Q two-step process. A: SDS-PAGE with Coomassie stain (SimpleBlue™ SafeStain); B: Western-blot image. Both images are from the identical gel with the same sample loading in each lane. Lane 1: molecular weight markers; lane 2: *E. coli* clarified lysate; lane 3: Partially purified OPN fraction from HEA HyperCel elute; lane 4: Dialyzed HEA purified fraction as the feed for Capto Q chromatography; lane 5: Capto Q elute pool. For lane 2-5, total protein loading was kept constant at 5 µg/lane.

**Table 7** Purification of OPN from *E. coli* lysate by HEA-Q 2-step process

Step	Volume (ml)	OPN (µg)	Purity (%)	Purification Fold	Recovery (%)
<b>Clarified Lysate feed</b>	4.2	465.1	1.9*	1.0	100
<b>HEA HyperCel</b>	5.6	378.2	29*	15.6	81
<b>Dialysis</b>	6.0	228.8	20*	0.7	49
<b>Capto Q</b>	1.50	202.8	95 (including fragments); 60 (full length OPN)**	3.5	44

\*Purity calculated from OPN concentration by ELISA and TP by Bradford assay.

\*\*Purity calculated by ImageJ software based on SDS-PAGE image.

### 3.2.2 OPN purification by Q-HEA process

The alternative 2-step process train used a reversed order of resins: CaptoQ capture followed by HEA purification. The clarified lysate was first dialyzed to conductivity of 5 mS/cm before loading onto Capto Q column. The chromatogram of the Capto Q capture step was the same previously shown and discussed in Figure 17. The pooled OPN fractions from Capto Q, which had a conductivity of 45 mS/cm ( about 0.4 M NaCl equivalent), was then diluted 3-fold to conductivity below 17 mS/cm for efficient adsorption to HEA HyperCel. The same step-change elution on HEA HyperCel was performed after 20 column volumes of wash as the capture step in previous process was used here as the second purification step.

The data for this purification process are summarized in Table 8. Capto Q captured OPN from conditioned lysate and purified OPN from 2% purity to 22% with 90% recovery and also reduced the volume by more than 2-fold. HEA HyperCel showed high specificity for elution pool from Capto Q and achieved 94% OPN purity by a single elution step. Overall, 50% recovery with 94% purity was achieved by this 2-step process (Table 8).

OPN loss during dialysis of crude lysate was negligible while dialysis on partially purified OPN from the previous process resulted in significant loss. This was probably because the membrane was partially fouled by the bulk *E. coli* protein in the lysate and prevented major OPN binding to the dialysis membrane.

The overall yield of Q-HEA process is slightly higher than HEA-Q process with the purity being identical. Therefore, the dynamic binding capacity of the two resins, and

the yield of diafiltration at larger scale are the deciding factors for which process is better for large scale manufacturing.

**Table 8** Purification of OPN from *E. coli* lysate by Q-HEA 2-step process

Step	Volume (ml)	OPN (µg)	Purity (%)	Purification fold	Recovery (%)
<b>Dialyzed Cell Lysate</b>	4.3	298.8	1.9*	1.0	100
<b>Capto Q</b>	2	268.0	22*	11.7	90
<b>HEA HyperCel</b>	3	151.3	94 (including OPN fragments); 79 (full length OPN)**	4.3	51

\*Purity calculated from OPN concentration by ELISA and TP by Bradford assay.

\*\*Purity calculated by ImageJ software based on SDS-PAGE image

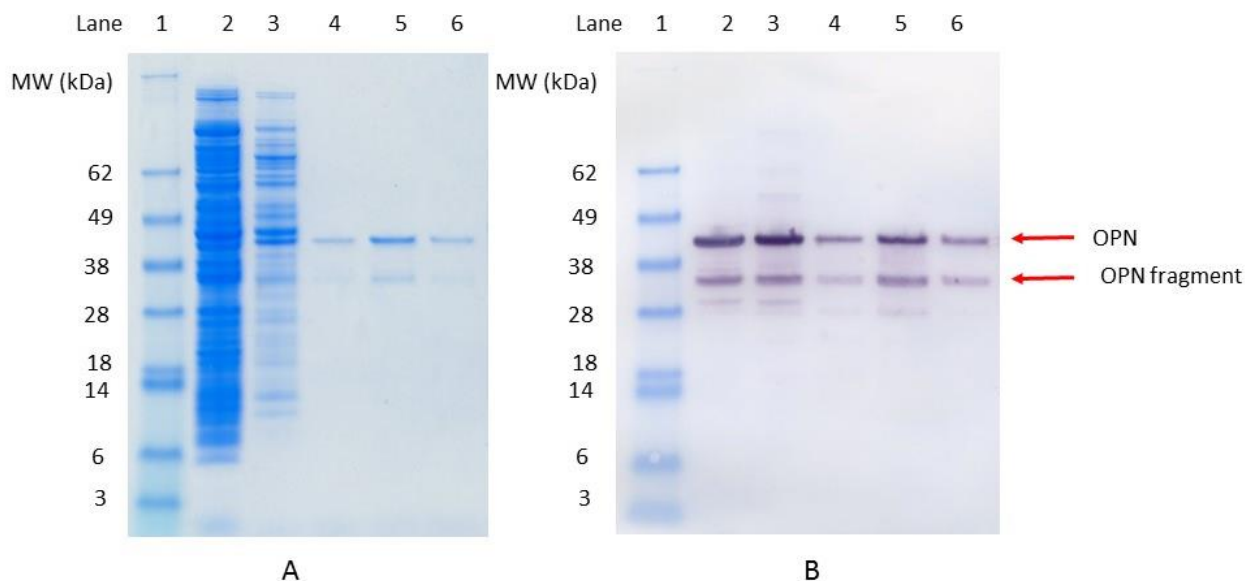


**Figure 21** Purification of OPN by Q-HEA process SDS-PAGE (A) with Coomassie stain (SimpleBlue™ SafeStain) and Western-blot ((B) images. Lane 1: molecular weight marker; lane 2: *E. coli* clarified lysate; lane 3: Partially purified OPN fraction from Capto Q elute; lane 4-6: OPN elute fractions from HEA HyperCel.

## 4 CONCLUSION AND RECOMMENDATIONS

### 4.1 Conclusion

This research focused on the chromatography resin screening and chromatography process development for OPN purification from *E. coli* lysate. The development process went from high-throughput and small scale testing in 96-well plates to fine-tuning each step on packed-bed columns.

A comprehensive investigation of four mixed-modal resins with hydrophobic and ionic characteristics revealed how subtle ligand chemistry differences affected OPN and *E. coli* HCPs adsorption. The four mixed-modal resins responded to variation of pH and salt concentration in a dramatically different fashion. Capto adhere, often categorized as a mixed-modal anion exchanger, behaved like a traditional anion exchanger and required low conductivity for efficient OPN adsorption. High ionic strength ( $> 0.5$  M NaCl) or low pH (pH 3) conditions led to OPN elution. Unfortunately, the added hydrophobic feature of Capto adhere ligand failed to translate into a better performance in the case of OPN purification. HEA HyperCel proved to be mixed-modal resin with seemingly an optimal combination of hydrophobic interaction and anion exchanger properties. Protein adsorption happened at both low salt and high salt concentration conditions. At low salt condition ( $< 0.5$  M NaCl), OPN was retained by electrostatic interaction as the ligand and OPN were oppositely charged. Also, the hydrophobic arm of the ligand appeared to help achieving salt-tolerant adsorption (efficient binding with 0.15 M NaCl). Interestingly, when the salt concentration in the adsorption buffer increased to higher than 2.5 M NaCl values, the hydrophobic interaction mechanism took over and exerted strong affinity for



OPN. A close sibling of HEA HyperCel, PPA HyperCel behaved similarly to HEA, but unfortunately the aromatic ring on PPA ligand made it too hydrophobic for OPN, so OPN could not be easily eluted from PPA comparing to HEA. MEP HyperCel adsorption, on the other hand, did not work in a mixed-modal way during adsorption since the ligand had little charge when the pH was above its pKa of 4.8. OPN could bind to MEP HyperCel via hydrophobic interaction but could not be eluted in a single fraction with a decent yield and purity.

Combination of batch adsorption and step elution experiments worked well as a resin performance evaluation and comparison method. Best performers could be easily identified by simple t-tests. The performance results from batch adsorption experiment were comparable to the results obtained with pre-packed columns operated by ÄKTA systems with much less time and buffer consumption.

The best two performing resins - HEA HyperCel and Capto Q - utilized different chemistries for OPN adsorption allowing development of orthogonal purification trains. The two purification options tested (HEA-Q and Capto Q –HEA) yielded similar recovery of close to 50% and OPN purity of 95%. HEA-Q process fully took advantage of the salt-tolerant adsorption feature of HEA to eliminate conditioning step on the crude lysate, which could be beneficial for large scale manufacturing. However, OPN loss during dialysis between chromatography steps needed to be addressed before moving forward with this process. The Q-HEA process exploit the chromatofocusing feature of traditional ion exchange resin Capto Q for significant volume reduction during the capture step. HEA HyperCel worked well as a second step to further purify OPN.

## 4.2 Recommendation

Suggestions for future work include:

- i. Determine the dynamic binding capacity of HEA HyperCel and Capto Q. Optimize the process to take advantage of the binding capacity of the two columns.
- ii. Develop a scalable diafiltration process for salt removal between the chromatography steps to eliminate OPN loss
- iii. Investigate viable bioseparation methods for OPN polishing step. An efficient polishing chromatography is required to remove OPN fragment and the remaining host cell protein should be removed in the polishing step.
- iv. Analyze the cell adhesion activity and other biochemical activities of purified OPN. Determine difference in activities of full length OPN and OPN fragment.

## REFERENCES

1. Senger, D. R.; Asch, B. B.; Smith, B. D.; Perruzzi, C. A.; Dvorak, H. F., A secreted phosphoprotein marker for neoplastic transformation of both epithelial and fibroblastic cells. *Nature* **1983**, *302* (5910), 714.
2. Franzen, A.; Heinegård, D., Isolation and characterization of two sialoproteins present only in bone calcified matrix. *Biochemical Journal* **1985**, *232* (3), 715-724.
3. Senger, D. R.; Perruzzi, C. A.; Papadopoulos, A.; Tenen, D. G., Purification of a human milk protein closely similar to tumor-secreted phosphoproteins and osteopontin. *Biochimica et Biophysica Acta (BBA)-Protein Structure and Molecular Enzymology* **1989**, *996* (1-2), 43-48.
4. Yuan, Y.; Zhang, X.; Weng, S.; Guan, W.; Xiang, D.; Gao, J.; Li, J.; Han, W.; Yu, Y., Expression and purification of bioactive high-purity recombinant mouse SPP1 in *Escherichia coli*. *Applied biochemistry and biotechnology* **2014**, *173* (2), 421-32.
5. Bayless, K. J.; Davis, G. E.; Meininger, G. A., Isolation and biological properties of osteopontin from bovine milk. *Protein expression and purification* **1997**, *9* (3), 309-314.
6. Kazanecki, C. C.; Uzwiak, D. J.; Denhardt, D. T., Control of osteopontin signaling and function by post-translational phosphorylation and protein folding. *Journal of cellular biochemistry* **2007**, *102* (4), 912-924.
7. Kurzbach, D.; Platzer, G.; Schwarz, T. C.; Henen, M. A.; Konrat, R.; Hinderberger, D., Cooperative unfolding of compact conformations of the intrinsically disordered protein osteopontin. *Biochemistry* **2013**, *52* (31), 5167-5175.

8. Fisher, L.; Torchia, D.; Fohr, B.; Young, M.; Fedarko, N., Flexible structures of SIBLING proteins, bone sialoprotein, and osteopontin. *Biochemical and biophysical research communications* **2001**, *280* (2), 460-465.
9. Kazanecki, C. C.; Uzwiak, D. J.; Denhardt, D. T., Control of osteopontin signaling and function by post-translational phosphorylation and protein folding. *J Cell Biochem* **2007**, *102* (4), 912-24.
10. Sørensen, E. S.; Petersen, T. E.; Højrup, P., Posttranslational modifications of bovine osteopontin: Identification of twenty-eight phosphorylation and three O-glycosylation sites. *Protein Science* **1995**, *4* (10), 2040-2049.
11. Christensen, B.; Nielsen, M. S.; Haselmann, K. F.; Petersen, T. E.; Sørensen, E. S., Post-translationally modified residues of native human osteopontin are located in clusters: identification of 36 phosphorylation and five O-glycosylation sites and their biological implications. *Biochemical Journal* **2005**, *390* (1), 285-292.
12. Heinegård, D.; Hultenby, K.; Oldberg, Å.; Reinholt, F.; Wendel, M., Macromolecules in bone matrix. *Connective Tissue Research* **2009**, *21* (1-4), 3-14.
13. Reinholt, F. P.; Hultenby, K.; Oldberg, A.; Heinegård, D., Osteopontin--a possible anchor of osteoclasts to bone. *Proceedings of the National Academy of Sciences* **1990**, *87* (12), 4473-4475.
14. McKee, M.; Nanci, A., Osteopontin at mineralized tissue interfaces in bone, teeth, and osseointegrated implants: ultrastructural distribution and implications for mineralized tissue formation, turnover, and repair. *Microscopy research and technique* **1996**, *33* (2), 141-164.

15. Butler, W. T., Matrix Macromolecules of Bone and Dentin. *Collagen and Related Research* **1984**, 4 (4), 297-307.
16. Kitahara, K.; Ishijima, M.; Rittling, S. R.; Tsuji, K.; Kurosawa, H.; Nifuji, A.; Denhardt, D. T.; Noda, M., Osteopontin deficiency induces parathyroid hormone enhancement of cortical bone formation. *Endocrinology* **2003**, 144 (5), 2132-40.
17. Kleinman, J. G.; Beshensky, A.; Worcester, E. M.; Brown, D., Expression of osteopontin, a urinary inhibitor of stone mineral crystal growth, in rat kidney. *Kidney International* **1995**, 47 (6), 1585-1596.
18. Hudkins, K. L.; Giachelli, C. M.; Cui, Y.; Couser, W. G.; Johnson, R. J.; Alpers, C. E., Osteopontin expression in fetal and mature human kidney. *Journal of the American Society of Nephrology* **1999**, 10 (3), 444-457.
19. Min, W.; Shiraga, H.; Chalko, C.; Goldfarb, S.; Krishna, G. G.; Hoyer, J. R., Quantitative studies of human urinary excretion of uropontin. *Kidney Int* **1998**, 53 (1), 189-93.
20. Lieske, J. C.; Leonard, R.; Toback, F. G., Adhesion of calcium oxalate monohydrate crystals to renal epithelial cells is inhibited by specific anions. *American Journal of Physiology-Renal Physiology* **1995**, 268 (4), F604-F612.
21. Yamate, T.; Tsuji, H.; Amasaki, N.; Iguchi, M.; Kurita, T.; Kohri, K., Analysis of osteopontin DNA in patients with urolithiasis. *Urological Research* **2000**, 28 (3), 159-166.
22. Atai, N. A.; Bansal, M.; Lo, C.; Bosman, J.; Tigchelaar, W.; Bosch, K. S.; Jonker, A.; De Witt Hamer, P. C.; Troost, D.; McCulloch, C. A., Osteopontin is up-

regulated and associated with neutrophil and macrophage infiltration in glioblastoma.

*Immunology* **2011**, *132* (1), 39-48.

23. Shevde, L. A.; Samant, R. S., Role of osteopontin in the pathophysiology of cancer. *Matrix Biology* **2014**, *37*, 131-141.

24. Rangaswami, H.; Bulbule, A.; Kundu, G. C., Osteopontin: role in cell signaling and cancer progression. *Trends Cell Biol* **2006**, *16* (2), 79-87.

25. Anborgh, P. H.; Mutrie, J. C.; Tuck, A. B.; Chambers, A. F., Pre-and post-translational regulation of osteopontin in cancer. *Journal of cell communication and signaling* **2011**, *5* (2), 111-122.

26. Cohen, S. N.; Chang, A. C.; Boyer, H. W.; Helling, R. B., Construction of biologically functional bacterial plasmids in vitro. *Proceedings of the National Academy of Sciences* **1973**, *70* (11), 3240-3244.

27. Pavlou, A. K.; Reichert, J. M., Recombinant protein therapeutics—success rates, market trends and values to 2010. *Nature biotechnology* **2004**, *22* (12), 1513-1519.

28. Altman, L. K., A new insulin given approval for use in US. *New York Times* **1982**, *30*.

29. Baeshen, M. N.; Al-Hejin, A. M.; Bora, R. S.; Ahmed, M.; Ramadan, H.; Saini, K. S.; Baeshen, N. A.; Redwan, E. M., Production of biopharmaceuticals in *E. coli*: current scenario and future perspectives. *J Microbiol Biotechnol* **2015**, *25* (7), 953-962.

30. Walsh, G., Biopharmaceutical benchmarks 2014. *Nature biotechnology* **2014**, *32* (10), 992.

31. Walsh, G.; Jefferis, R., Post-translational modifications in the context of therapeutic proteins. *Nature biotechnology* **2006**, *24* (10), 1241.
32. Jang, J. H.; Kim, J. H., Improved cellular response of osteoblast cells using recombinant human osteopontin protein produced by Escherichia coli. *Biotechnology letters* **2005**, *27* (22), 1767-70.
33. Ashkar, S.; Teplow, D.; Glimcher, M.; Saavedra, R., In vitro phosphorylation of mouse osteopontin expressed in E. coli. *Biochemical and biophysical research communications* **1993**, *191* (1), 126-133.
34. GE Healthcare Lifesciences, Hydrophobic Interaction Chromatography (HIC) Selection Guide. **2012**.
35. Gagnon, P., IgG aggregate removal by charged-hydrophobic mixed mode chromatography. *Current pharmaceutical biotechnology* **2009**, *10* (4), 434-439.
36. Ghose, S.; Hubbard, B.; Cramer, S. M., Evaluation and comparison of alternatives to Protein A chromatography Mimetic and hydrophobic charge induction chromatographic stationary phases. *Journal of chromatography. A* **2006**, *1122* (1-2), 144-52.
37. Guerrier, L.; Flayeux, I.; Boschetti, E., A dual-mode approach to the selective separation of antibodies and their fragments. *Journal of Chromatography B: Biomedical Sciences and Applications* **2001**, *755* (1), 37-46.
38. Pezzini, J.; Joucla, G.; Gantier, R.; Toueille, M.; Lomenech, A. M.; Le Senechal, C.; Garbay, B.; Santarelli, X.; Cabanne, C., Antibody capture by mixed-mode chromatography: a comprehensive study from determination of optimal purification

- conditions to identification of contaminating host cell proteins. *Journal of chromatography. A* **2011**, *1218* (45), 8197-208.
39. Arakawa, T.; Futatsumori-Sugai, M.; Tsumoto, K.; Kita, Y.; Sato, H.; Ejima, D., MEP HyperCel chromatography II: binding, washing and elution. *Protein expression and purification* **2010**, *71* (2), 168-73.
40. Brenac Brochier, V.; Chabre, H.; Lautrette, A.; Ravault, V.; Couret, M. N.; Didierlaurent, A.; Moingeon, P., High throughput screening of mixed-mode sorbents and optimisation using pre-packed lab-scale columns for the purification of the recombinant allergen rBet v 1a. *J Chromatogr B Analyt Technol Biomed Life Sci* **2009**, *877* (24), 2420-7.
41. Coulon, D.; Cabanne, C.; Fitton, V.; Noubhani, A. M.; Saint-Christophe, E.; Santarelli, X., Penicillin acylase purification with the aid of hydrophobic charge induction chromatography. *Journal of chromatography. B, Analytical technologies in the biomedical and life sciences* **2004**, *808* (1), 111-5.
42. Brenac Brochier, V.; Schapman, A.; Santambien, P.; Britsch, L., Fast purification process optimization using mixed-mode chromatography sorbents in pre-packed mini-columns. *J Chromatogr A* **2008**, *1177* (2), 226-33.
43. Cabanne, C.; Pezzini, J.; Joucla, G.; Hocquellet, A.; Barbot, C.; Garbay, B.; Santarelli, X., Efficient purification of recombinant proteins fused to maltose-binding protein by mixed-mode chromatography. *J Chromatogr A* **2009**, *1216* (20), 4451-6.
44. Zhao, G.; Dong, X. Y.; Sun, Y., Ligands for mixed-mode protein chromatography: Principles, characteristics and design. *J Biotechnol* **2009**, *144* (1), 3-11.



45. Hou, Y.; Cramer, S. M., Evaluation of selectivity in multimodal anion exchange systems: a priori prediction of protein retention and examination of mobile phase modifier effects. *Journal of chromatography. A* **2011**, *1218* (43), 7813-20.
46. Nfor, B. K.; Noverraz, M.; Chilamkurthi, S.; Verhaert, P. D.; van der Wielen, L. A.; Ottens, M., High-throughput isotherm determination and thermodynamic modeling of protein adsorption on mixed mode adsorbents. *Journal of chromatography. A* **2010**, *1217* (44), 6829-50.
47. Zhao, G.; Dong, X.-Y.; Sun, Y., Ligands for mixed-mode protein chromatography: principles, characteristics and design. *Journal of biotechnology* **2009**, *144* (1), 3-11.
48. Sørensen, S.; Justesen, S. J.; Johnsen, A. H., Purification and characterization of osteopontin from human milk. *Protein Expression and Purification* **2003**, *30* (2), 238-245.
49. Azuma, N.; Maeta, A.; Fukuchi, K.; Kanno, C., A rapid method for purifying osteopontin from bovine milk and interaction between osteopontin and other milk proteins. *International Dairy Journal* **2006**, *16* (4), 370-378.
50. Hwang, S.; Lopez, C. A.; Heck, D. E.; Gardner, C. R.; Laskin, D. L.; Laskin, J. D.; Denhardt, D. T., Osteopontin inhibits induction of nitric oxide synthase gene expression by inflammatory mediators in mouse kidney epithelial cells. *Journal of Biological Chemistry* **1994**, *269* (1), 711-715.

51. Xuan, J. W.; Hota, C.; Chambers, A. F., Recombinant GST-human osteopontin fusion protein is functional in RGD-dependent cell adhesion. *Journal of cellular biochemistry* **1994**, *54* (2), 247-255.
52. Rollo, E. E.; Laskin, D. L.; Denhardt, D. T., Osteopontin inhibits nitric oxide production and cytotoxicity by activated RAW264. 7 macrophages. *Journal of leukocyte biology* **1996**, *60* (3), 397-404.
53. Bradford, M. M., A rapid and sensitive method for the quantitation of microgram quantities of protein utilizing the principle of protein-dye binding. *Analytical biochemistry* **1976**, *72* (1-2), 248-254.

## APPENDIX

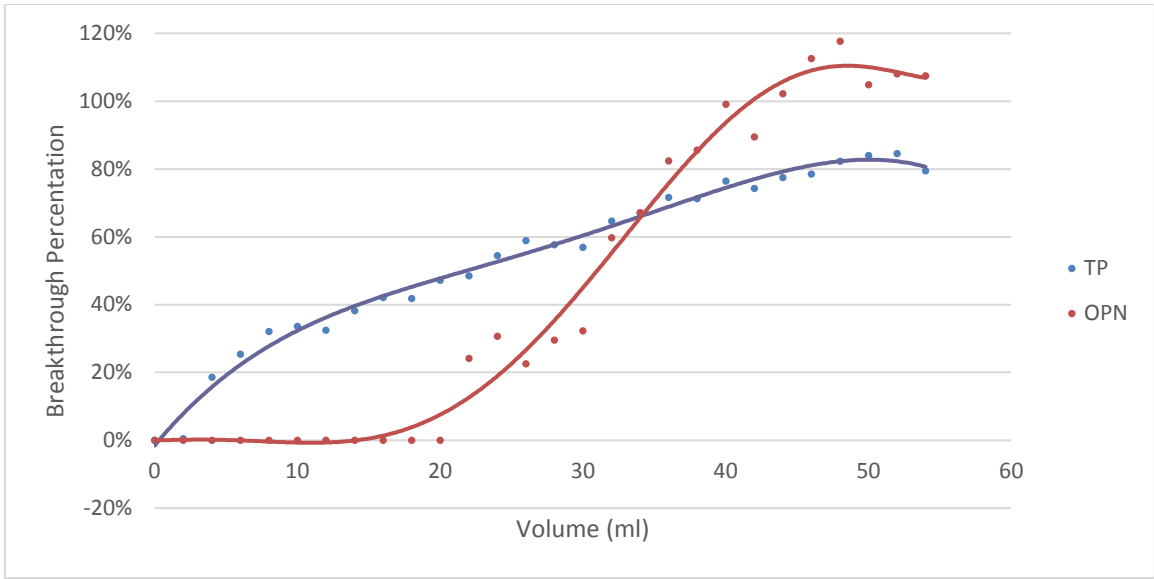
### **Dynamic binding capacity determination**

Dynamic binding capacity (DBC) is one of the most important parameter in chromatography process development, especially for the capture step. However, with the presence of a large variety and quantity of impurities, DBC could not be easily translated from batch adsorption data. Experimental determination of DBC were conducted by constant loading the feed material onto packed-bed column, sampling the flowthrough and plot a breakthrough curve.

In the case of this study, both HEA HyperCel and Capto Q resins were capable of being the capture step for OPN purification from a separation power perspective. Therefore, DBC of the two resins could be the deciding factor of which resin serves better as the capture step for OPN purification.

#### *HEA HyperCel breakthrough curve*

Clarified lysate was loaded to pre-equilibrated PRC HEA HyperCel column (1 ml) at 60 cm/h linear velocity and the flowthrough were collected in 2 ml fraction samples.



**Supplementary Figure 1 Breakthrough Curve of OPN on HEA HyperCel**